1.0

1.1

1.25 1.4 1.6

1.8

2.0

2.2

2.5

2.8

3.2

3.6

4.0

4.5

5.0

MICROCOPY RESOLUTION TEST CHART

NATIONAL BUREAU OF STANDARDS-1963-A

THE UNIVERSITY OF ROCHESTER

THE INSTITUTE OF OPTICS

ROCHESTER, NEW YORK

LEVEL#

Optical Interference Coatings
for the Ultraviolet
Final Progress Report
covering the period

August 1, 1977 to July 31, 1978

Research Contract N00014-77-C-0573

Office of Naval Research

1030 East Green Street

Pasadena, California 91106

Principal Investigator:

Philip Baumeister
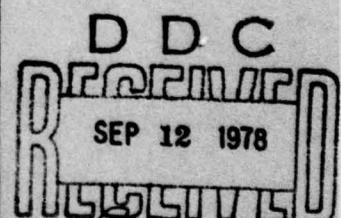
78 07 24 028

Optical Interference Coatings for the Ultraviolet.

Final Progress Report. 1 Aug 77-31 Jul 78,

covering the period

August 1, 1977 to July 31, 1978

Research Contract N00014-77-C-0573 *new*

with

Office of Naval Research

31 Jul 78

1030 East Green Street

Pasadena, California 91106

56p.

under the auspices of
Naval Weapons Center
Michelson Laboratory
China Lake, California
Principal Investigator: P.W. Baumeister

The Institute of Optics
University of Rochester
Rochester, New York 14627

Philip W./Baumeister

182 250

78 07 24 028

ABSTRACT

All dielectric multilayer reflectors were
constructed with a radiant reflectance R in excess
of 99% at a wavelength of 250 nm. The stacks contained
the following materials: hafnia, silica, magnesium
fluoride, and yttria.

Reflectors were also prepared using alternate layers
of silica and hafnia. A maximum reflectance in excess
of 0.995 was obtained at 355 nm.

Spectroreflectometry was used to determine the
refractive index versus wavelength of the following
optical coating materials: hafnia, yttria, lanthanum
sesquioxide, and tantalum pentoxide. All of these
materials, with the exception of the latter, are
optically transparent to wavelengths as short as 250 nm.

Table of contents

II. Experimental procedures

2.1 Introduction

Our objective was to deposit multilayer reflectors for the ultraviolet region by vacuum evaporation. An existing evaporation tank was refitted and re-instrumented as follows: (1) Re-installation of the ultraviolet optical monitoring system; and (2) Installation of improved substrate heaters and temperature control.

2.2 Description of coating apparatus

The UV coatings are deposited in a vacuum tank that is 0.76 m in diameter by 1.52 m in height.

Figure 1 shows the coating chamber and associated optical monitoring system. The hydrogen lamp $\underline{H}$ is imaged by quartz lenses L on the slit of the grating monochromator $\underline{G}$. The flux is directed through a mechanical chopper C, through the window $\underline{W}$ into the tank and thence upon the rotary holder that positions a quartz monitoring plate P in the beam. The reflected flux is then directed towards the exit window W and the monochromator. The only precaution is to insert an absorbing filter (Schott UG series) to reduce the scattered flux in the grating monochromator. The selection of the wavelength for optical monitoring is discussed below. The electrical signal from a 1P-28 photomultiplier (detector D) is fed into an amplifier and thence into a strip chart recorder.

Fig. 1
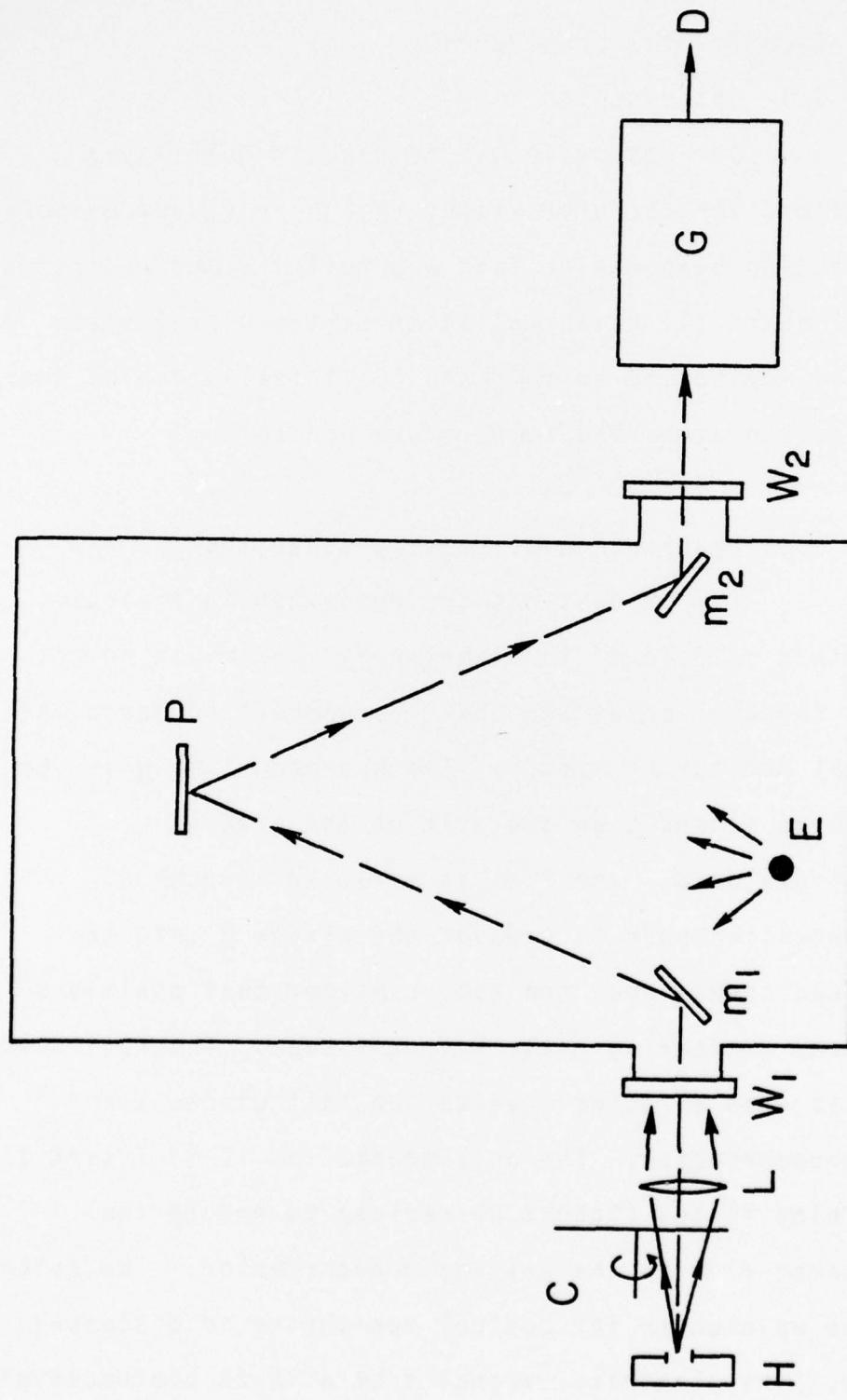
The evaporator used for the deposition of thin layers.

Elstein type radiation heaters were installed to heat the substrates during deposition. The heaters were positioned at a distance of approximately 15 cm from the substrates. The Elstein heaters have the advantage that they operate at a relatively low temperature and hence a substantial part of the radiation is absorbed by the silica substrates. The temperature is monitored with a thermocouple that is enclosed in a glass tube so that the transfer of radiant energy approximates that of the substrate.

2.3 Optical monitoring

The optical thicknesses of the layers were monitored optically by halting the deposition when the radiant reflectance reached a maximum or minimum. This produces quarterwave optical thickness layers.

Because of the nonnormal incidence of the flux upon the monitoring plate, the wavelength of the monochromator must be set at a wavelength that is about 7.5% shorter than the wavelength where a quarterwave optical thickness is desired. For example, if a film with a quarterwave optical thickness at 355 nm is desired, the monochromator is set at 324 nm. This posed no problems at 355 nm. But when the layers were deposited at the shorter wavelength of 250 nm, electrical signals from the 1P-28 dropped to low enough levels that the noise hindered the accurate

measurement of the maxima and minima of the reflectance versus time. This was solved by monitoring at a longer wavelength and using a rotating sector, as described below.

Three substrates were held in a jig that was rotated during deposition. A wedged-shaped mask was positioned underneath which covered the substrates during a fraction of each revolution. The effect was to produce a coating on the substrates that was thinner than the optical monitor plates. All of the mirrors at 250 nm were coated by this technique.

2.4 Optical coating materials and deposition

The following optical coating materials were considered for the dielectric mirrors:

OXIDES   FLUORIDES

aluminum oxide   ceric fluoride

hafnium dioxide   lanthanum fluoride

lanthanum oxide   magnesium fluoride

scandium oxide

silica

tantalum pentoxide

thorium dioxide

yttrium oxide

zirconium dioxide

Most of the foregoing materials are relatively transparent at 350 nm -- with the possible exception of tantalum pentoxide. Yttria and lanthanum oxide have relatively lower refractive indices and consequently more layers are needed to produce a given reflectance, as compared to the other materials.

Thoria is refractory in the extreme and difficult to evaporate, as well as being slightly radioactive. Since we have more experience in depositing layers of HfO_2, we decided to use HfO_2 and SiO_2 as the high and low index materials in the multilayer reflectors [1].

The former material was prepared for vacuum evaporation by the Merck Company. The hot-pressed tablets of HfO_2 were deposited with the electron gun at 1.1 KW power. The deposition of the granules of SiO_2 required only one-quarter of that power. The base pressure in the chamber was reduced to less $5 \ 10^{-6}$ torr before evaporation. Oxygen was re-addmitted to raise the pressure to $5 \ 10^{-5}$ torr. This assisted in oxydizing the evaporants more fully.

The fused silica, SiC, or Mo substrates were heated with the radiant heaters described earlier. The heat transfer from the heaters to the substrates is via radiant flux, principally in the infrared. An indication of the substrate temperature is obtained from a thermocouple that is encased in a glass tube. Since the infrared absorption of glass and the fused silica are very nearly the same, the thermocouple temperature is close to that of the bulk temperature of the fused silica. The surface

temperature of the fused silica, however, may be considerably higher than the bulk, due to the heat of sublimation of the evaporant. A temperature in the range $200^{\circ}C$ to $250^{\circ}C$ was used in all of the evaporations. The higher temperature is needed to oxydize the evaporants. The Mo substrates, on the other hand, absorb considerably less flux from the heaters and were undoubtedly considerably cooler than this 200 C. This is desirable, because the differential thermal expansion coefficients between the coating and metal substrates can cause severe mechanical stress.

The yttria was obtained in tablet form from the Cerac Corp. A thin skin at the surface of the evaporant melted during its deposition with an electron beam. At the conclusion of an evaporation, however, the tablets had crumbled to a powder and hence could not be reused. The same technique of bleeding in oxygen was used for the Y_2O_3, as for the HfO_2.

A relatively slow evaporation rate was used for the Y_2O_3. The indicated rate was 0.3 nm (physical thickness) per second. The *indicated* in the previous sentence means that we are not certain about the physical density of the yttria films, since the density must be known to calibrate the quartz crystal microbalance that was used to determine the rate.

2.5 Stabilization by baking

As mentioned in a previous section, the oxide materials were deposited onto substrates that were

relatively hot (250°C) and in a residual oxygen atmosphere.
Several investigations [2,3] have shown that the residual
oxygen and higher temperature produces films with nigher
refractive indices and lower optical absorption.

Both multilayer mirrors and single layers were
deposited. The refractive index of the latter were
determined as outlined in 3.1. The single layers were
baked to reduce the absorption still further via more
complete oxidation. The films were initially removed from
the evaporation chamber and the reflectance and transmittance
were measured via the procedure listed in section 3.2.
The black paint was then removed from the uncoated side
of the substrate and films were inserted in a furnace
and baked at 400°C in air for approximately 14 hours.

After removal from the furnace, they were allowed
to stabilize at room temperature for at least two days.
This allowed water vapor and other contaminants to come
to equilibrium with the matrix of the film. The radiant
reflectance and transmittance were then redetermined.
The effect of baking is discussed further in 3.4.

2.6 Reflectance and transmission measurements
The radiant reflectance R and transmittance T
were measured for several reasons: (a) To determine the
refractive index versus wavelength of the coating
materials; and, (b) To determine the reflectance and
losses in multilayer mirrors.

It is well known that $R \neq 1-T$ for so-called "dielectric" mirrors due to scattering and absorption losses. The reflectance was measured by the V-W attachment on the Cary model 14 spectrophotometer. It should be emphasized that the precision is limited to $\pm 0.5\%$. The experimental uncertainty should be kept in mind when some of the spectral reflectance curves in future sections are observed. Some of the coatings manifest reflectances in excess of 99.5%. It would have been presumptuous to claim that R actually attained a value of 99.8%. There is evidence that it exceeded 99.5%.

3.   Optical properties of materials

   3.1 Introduction

        Little is known about the refractive index versus wavelength of many of the coating materials cited in 2.4. We measured their refractive indices under the evaporation conditions that we had used. The refractive index data, along with the extinction coefficients, will enable the user to compute precisely the reflectance and transmittance versus wavelength of bandpass filters, multilayer polarizers and mirrors composed of these oxides and fluorides.

   3.2 Deposition and measurements

        We assumed that the dielectric films could be characterized as optically homogeneous materials that had a refractive index $\underline{n}$ and an extinction coefficient $\underline{k}$

written in terms of the complex optical constant n-ik.
The following procedure was used to determine n and k
as a function of wavelength.

    (a) The film was deposited upon a fused silica
          substrate, as described in section 2.

    (b) After its removal from the vacuum it was
          allowed to sit in ambient atmosphere for
          approximately eight hours to absorb water
          vapor and thus attain equilibrium in its
          optical properties.

    (c) The reflectance and transmittance were then
          measured on a Cary 14 spectrophotometer.

The next section describes how the R and T were
translated into n and k values.

3.3 Data reduction

The first step was to correct for the transmission
loss at the nonobverse side of the substrate. The
transmittance of the film T_f is

$$T_f \cong T_m \frac{(1 - R)}{1 + R(1 - T_m)} \qquad (1)$$

where R is the radiant reflectance at the air-substrate
interface and T_m is the measured transmittance. This
equation is derived in section 5. The uncoated side of

the substrate was blackened after the transmission
measurements had been made. This blackening suppressed
the unwanted Fresnel reflection from the nonobverse
side of the substrate. The density on the chart recorder
was fed directly into a computer program that found the
best fit by a regression technique. The following
equation was used for R

$$R = \frac{a_0 \cos^2\beta + a_2 \sin^2\beta}{a_1 \cos^2\beta + a_3 \sin^2\beta} \qquad (2)$$

where

$$a_0 = (n_0 - n_s)^2 \qquad (3)$$

$$a_1 = (n_0 + n_s)^2 \qquad (4)$$

$$a_2 = (n - n_0 n_s/n)^2 \qquad (5)$$

$$a_3 = (n + n_0 n_s/n)^2 \qquad (6)$$

$$\beta = 2\pi\sigma \, nh \qquad (7)$$

where $\underline{n_0}$, $\underline{n_s}$, and $\underline{n}$ are the refractive indices of the
incident medium, substrate, and film, respectively.
$\underline{h}$ is the metric thickness of the film and σ is the
vacuum wavenumber of the incident flux.

A Sellmaier type dispersion equation was assumed
for the film index:

$$n^2 = A + B \sigma^2 \quad . \tag{8}$$

The regression algorithm adjusted the constants A and B
in the foregoing equation, as well as the metric thickness,
until the defect function was minimized.

3.4 Refractive index

Figures 2 to 9 plot the radiant reflectance
and the transmittance of four of the oxides that were
coated in this study. These include hafnium dioxide,
yttrium sesquioxide, tantalum pentoxide and lanthanum
sesquioxide.

The spectral reflectance and transmittance, both
before and after the baking process, are depicted on the
same graph for comparison. One of the main features is
that the baking reduces the maximum reflectance. This
is evidence that the refractive index was decreased by
the baking. Another feature is a decrease in the
transmittance at the ultraviolet wavelength where the film
has a substantial absorption.

Figures 10, 11, 12 and 13 depict the computed
refractive index for the four metal oxides that were
studied.

Table 3-1 shows the computed fit to the coefficients
in the Sellmaier dispersion polynomial. As mentioned
earlier, in almost all cases, the baking decreased the
refractive index. This is manifested in Table 3-1 by

Figures 2 through 9

The measured reflectance $\underline{R}$ and transmittance $\underline{T}$ for films of hafnium dioxide, yttrium sesquioxide, tantalum pentoxide, and lanthanum sesquioxide, respectively. The solid curve is the prebake measurement. The broken curve is the film after baking for 14 hours at 400°C in air.

Fig. 2

Fig. 3

Fig. 4

Yttrium oxide

Fig. 5

Fig.6

Fig.7

Lanthanum oxide
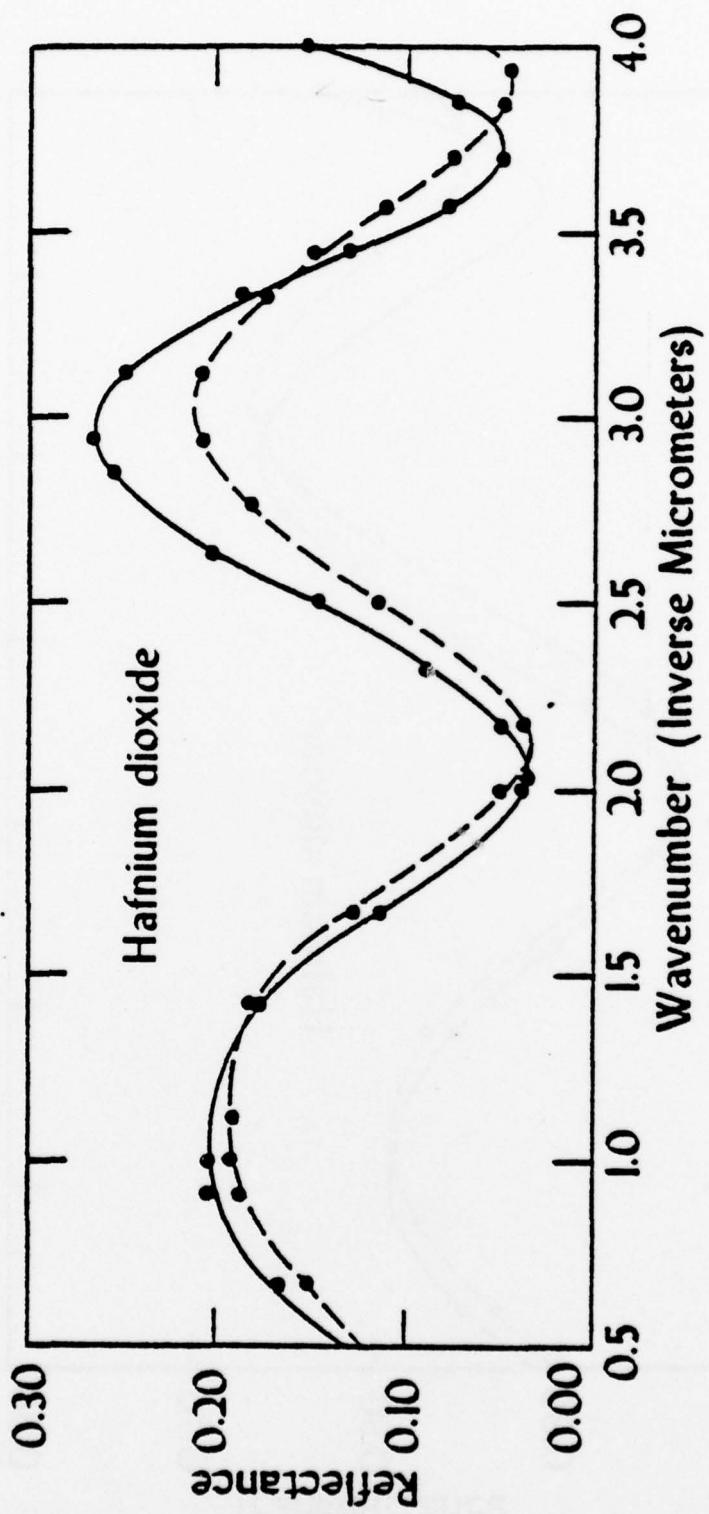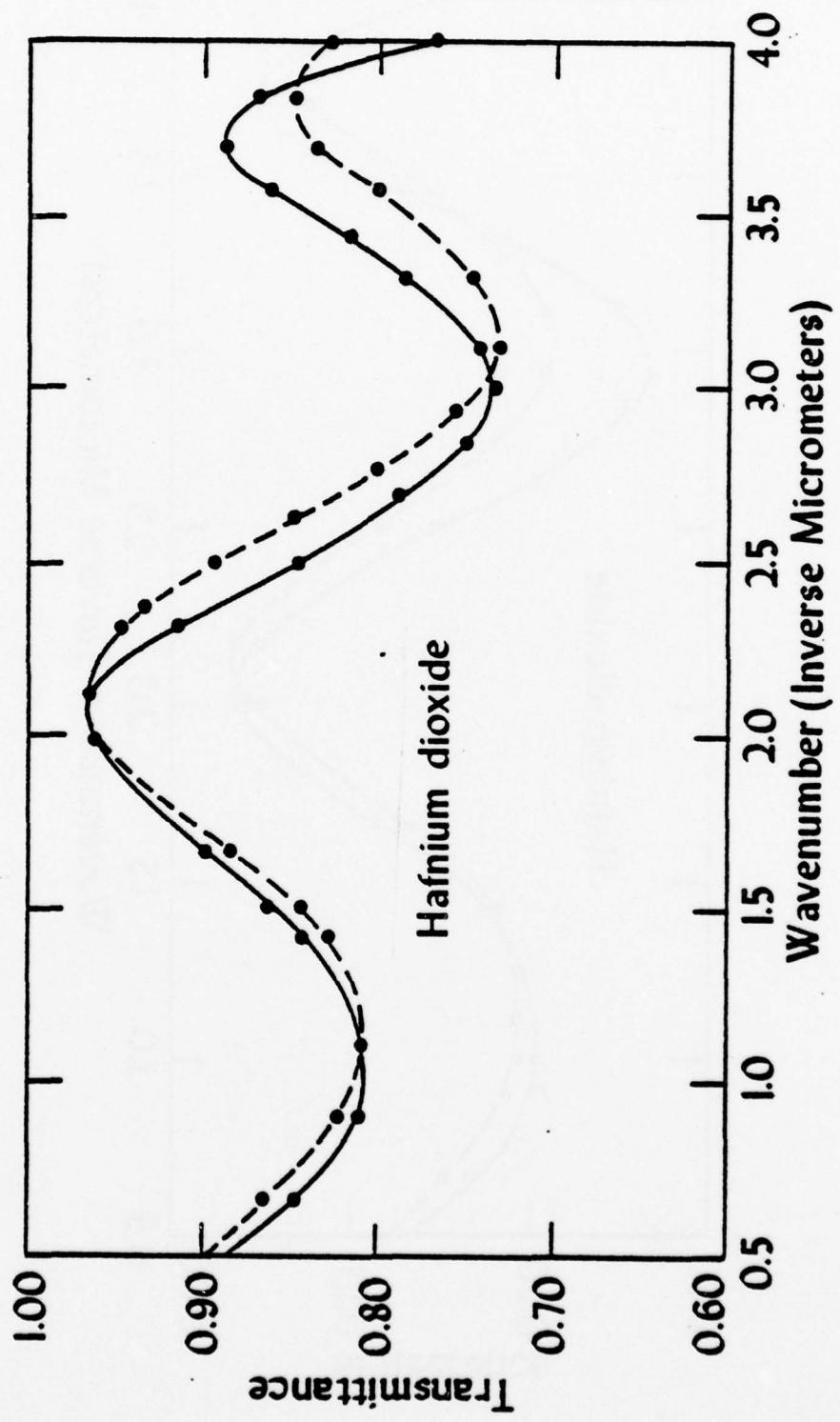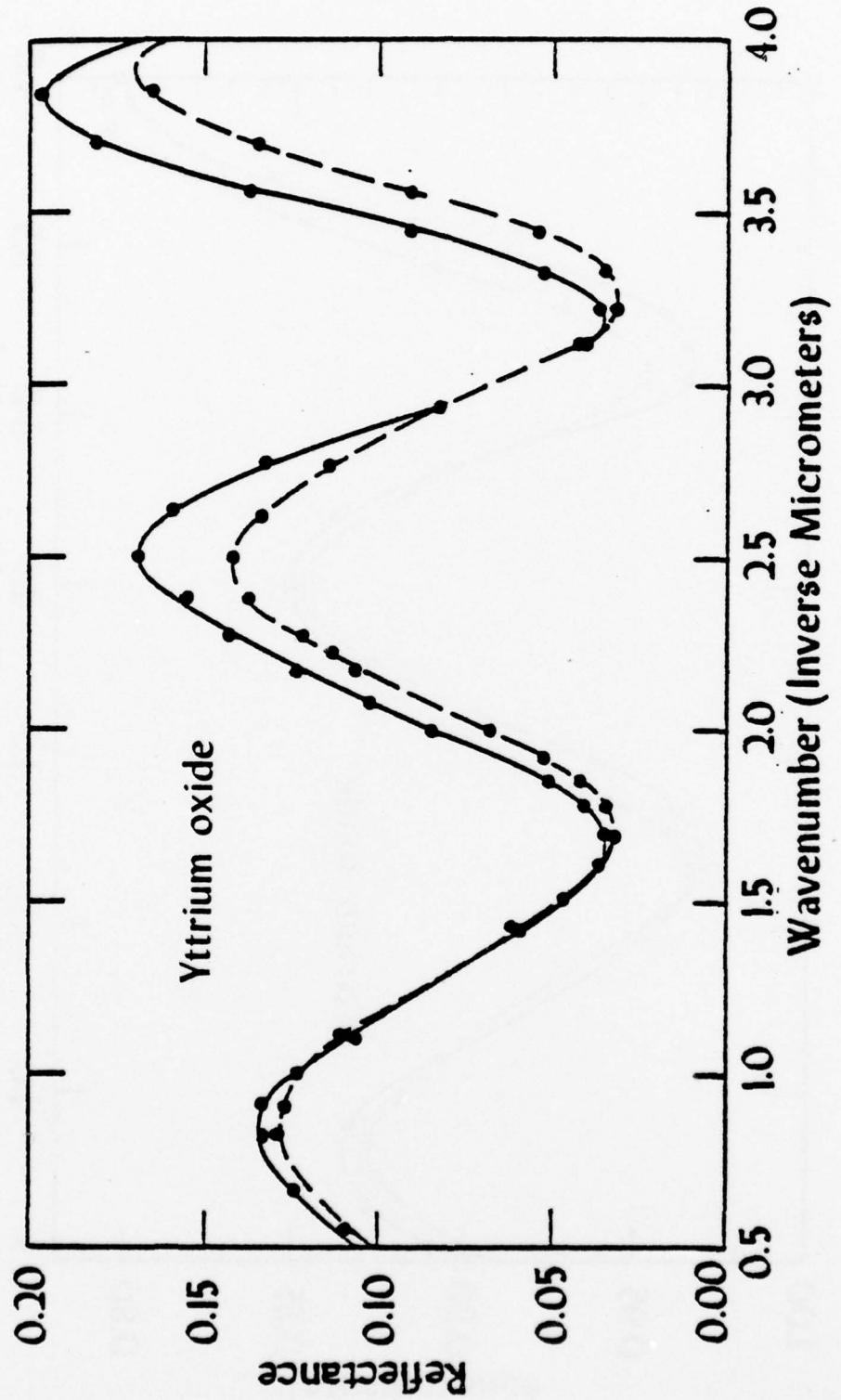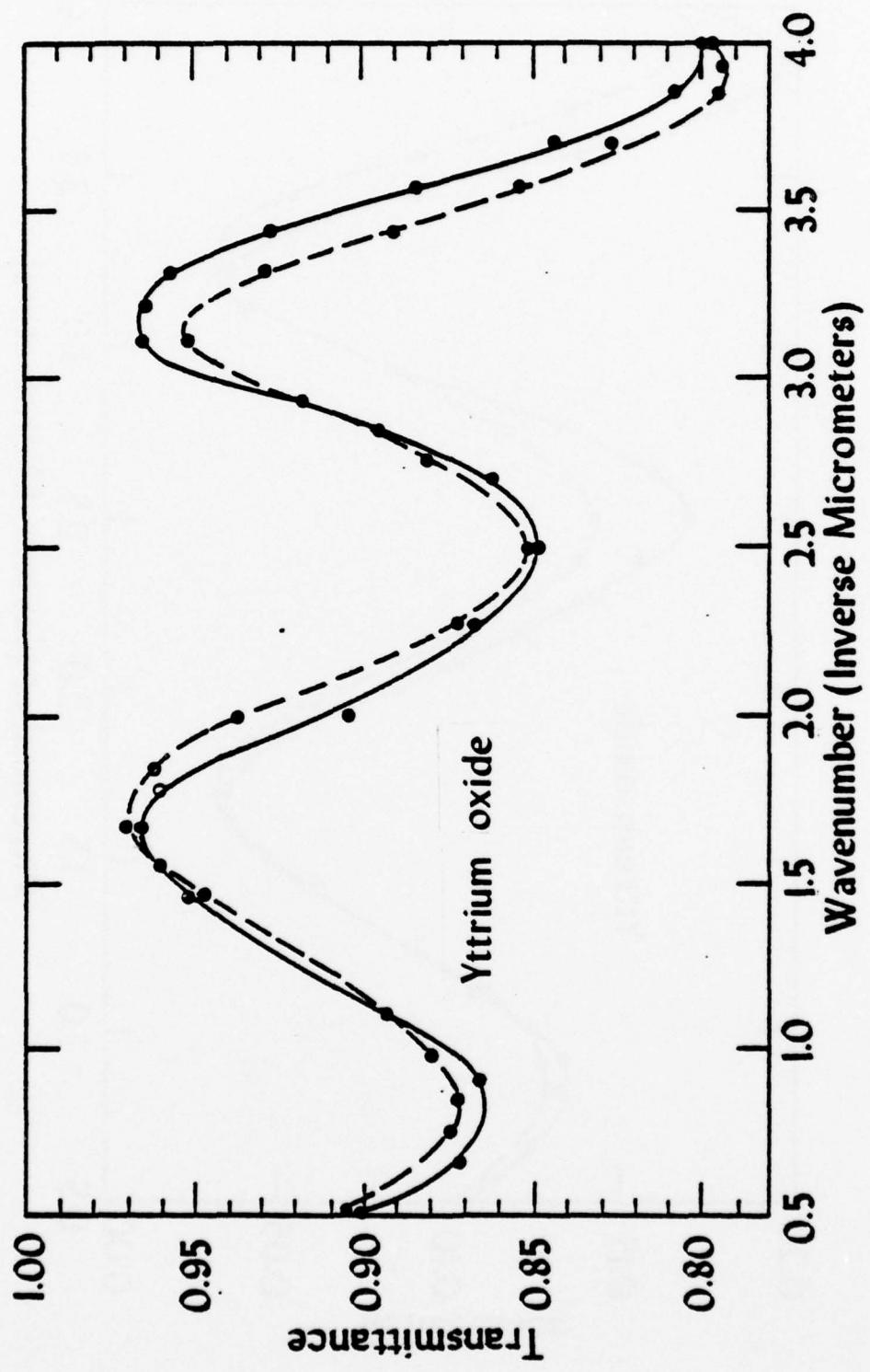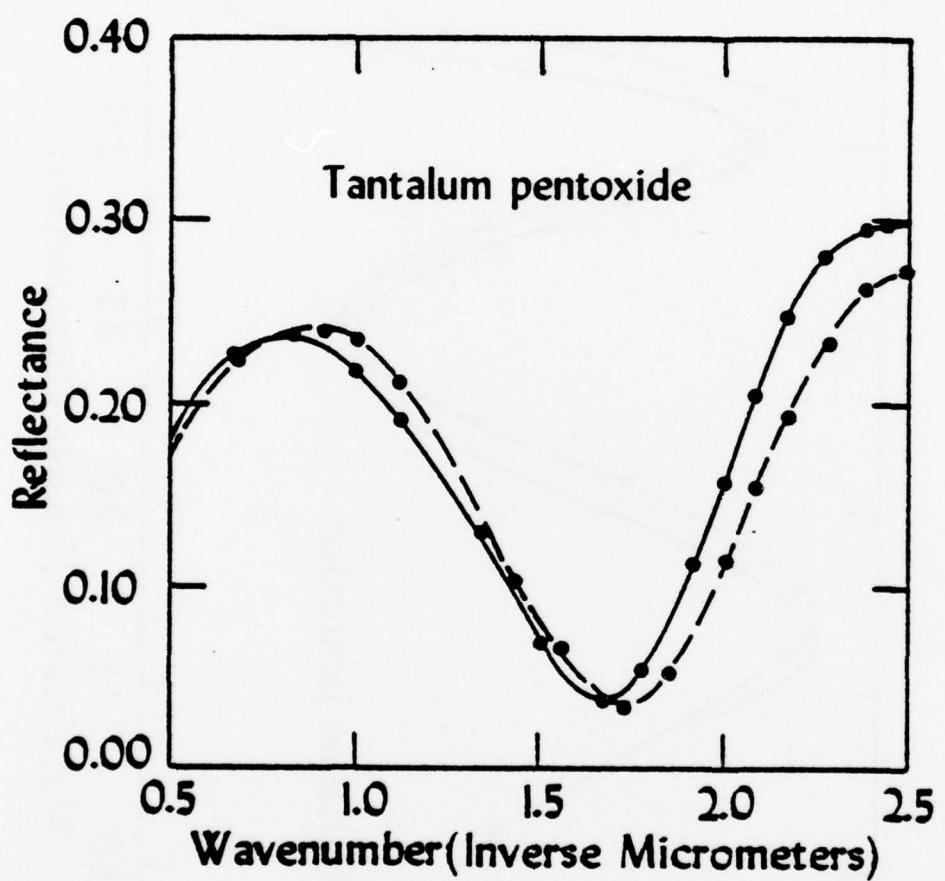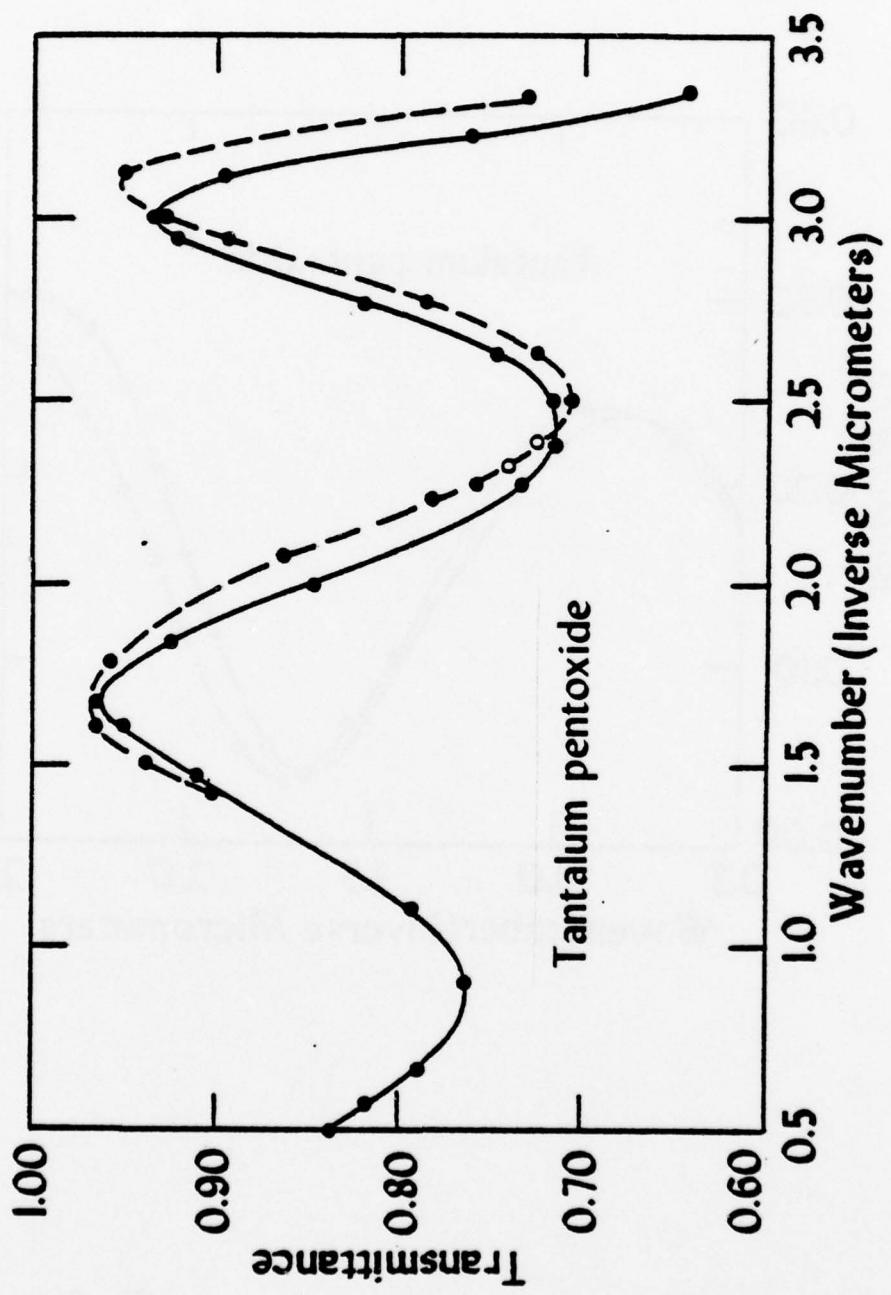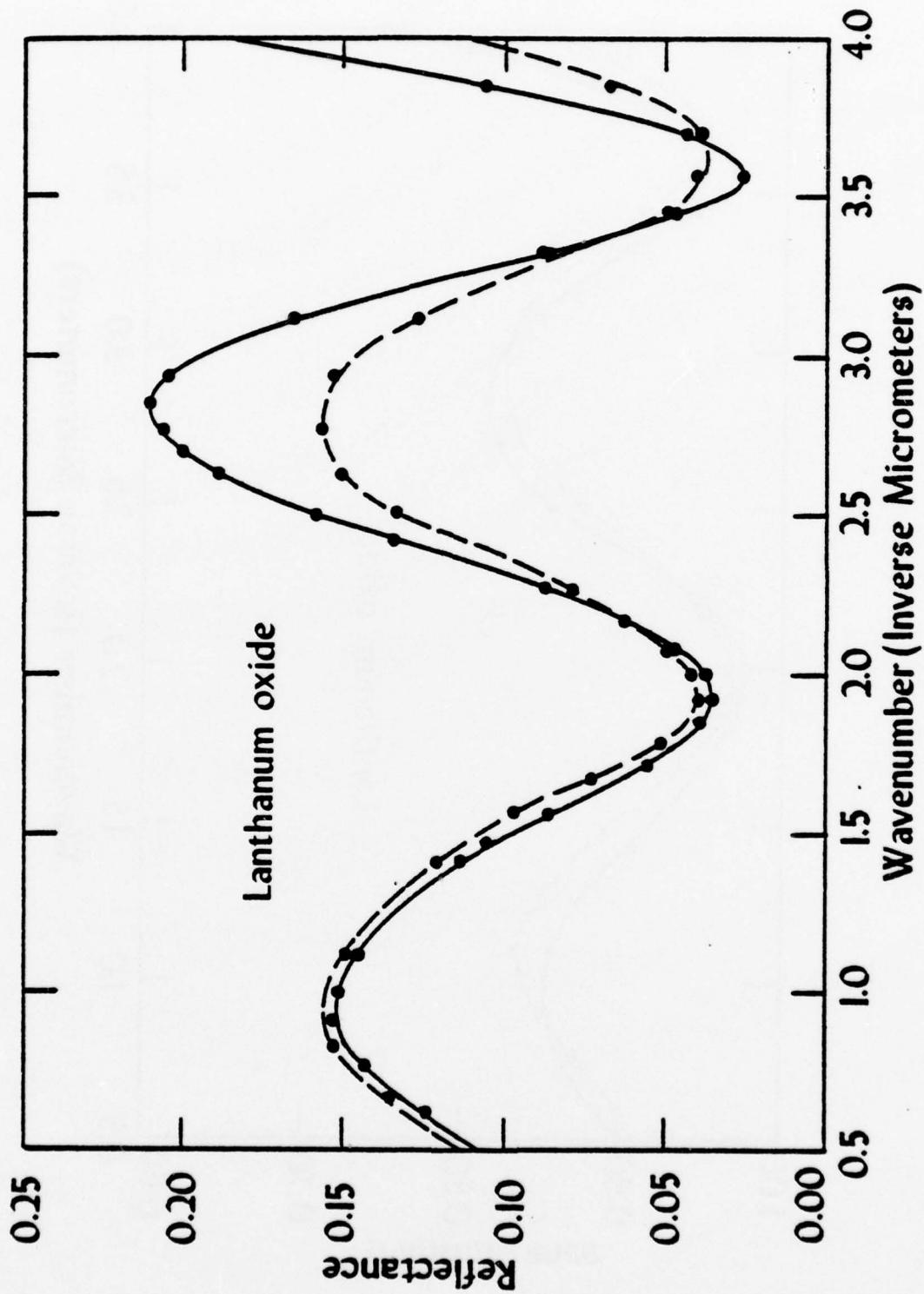
Fig. 8
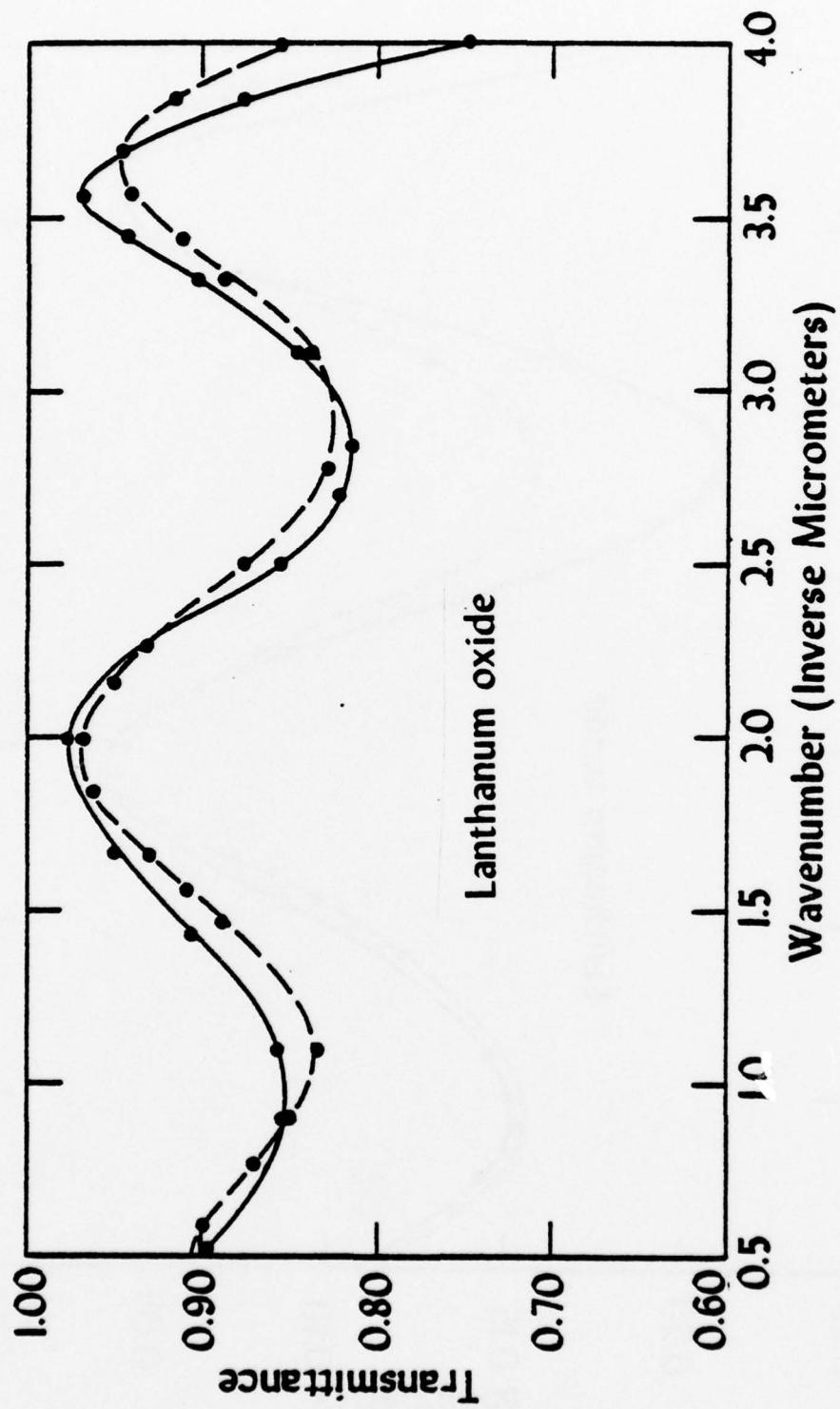
Fig. 9

Table 3-1

The optical parameters as determined by the computer

Material	Prebake			Postbake		
	A	B	h in μm	A	B	h in μm
HfO_2	3.8524	0.09188	0.118	3.7467	0.04687	0.120
Y_2O_3	3.1286	0.04195	0.165	3.0322	0.03089	0.170
Ta_2O_5	4.2446	0.13158	0.140	4.2454	0.06677	0.140
La_2O_3	3.3087	0.06952	0.137	3.3723	0.0197	0.142

The least squares determination of the metric thickness h and
the dispersion of the refractive index (where the constants A
and B appear in Eq. (8) via spectroreflectometry. Postbake
refers to baking at 14 h at 400°C in air.

Figures 10 through 13

The refractive index, as computed from
spectroreflectrometric data, for hafnium dioxide,
yttrium sesquioxide, tantalum pentoxide, and lanthanum
sesquioxide, respectively. Curve <u>a</u> corresponds to the
prebake measurements. Curve <u>b</u> is after baking at 400°C
in air for 14 hours.

Fig. 10

Fig. 11
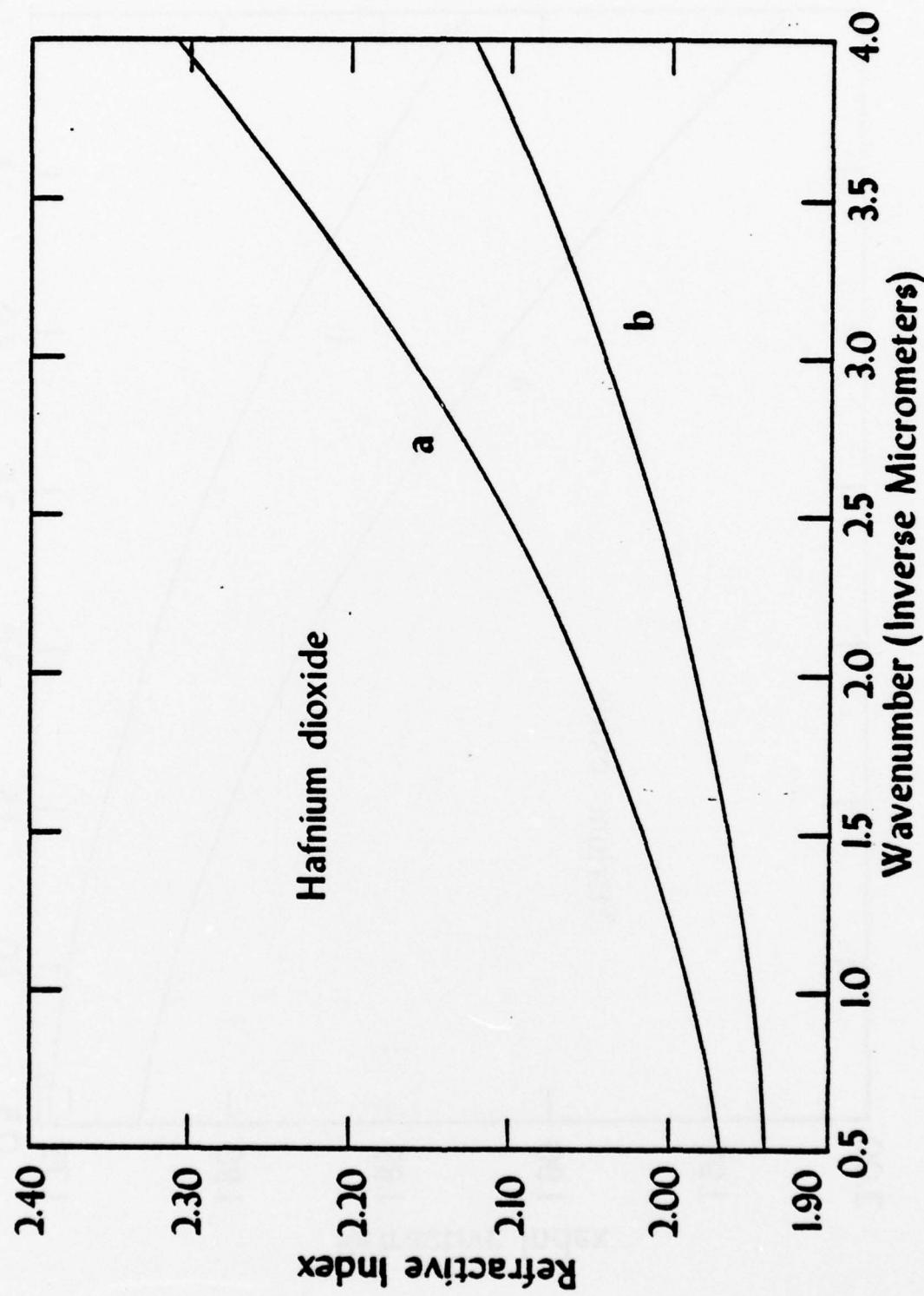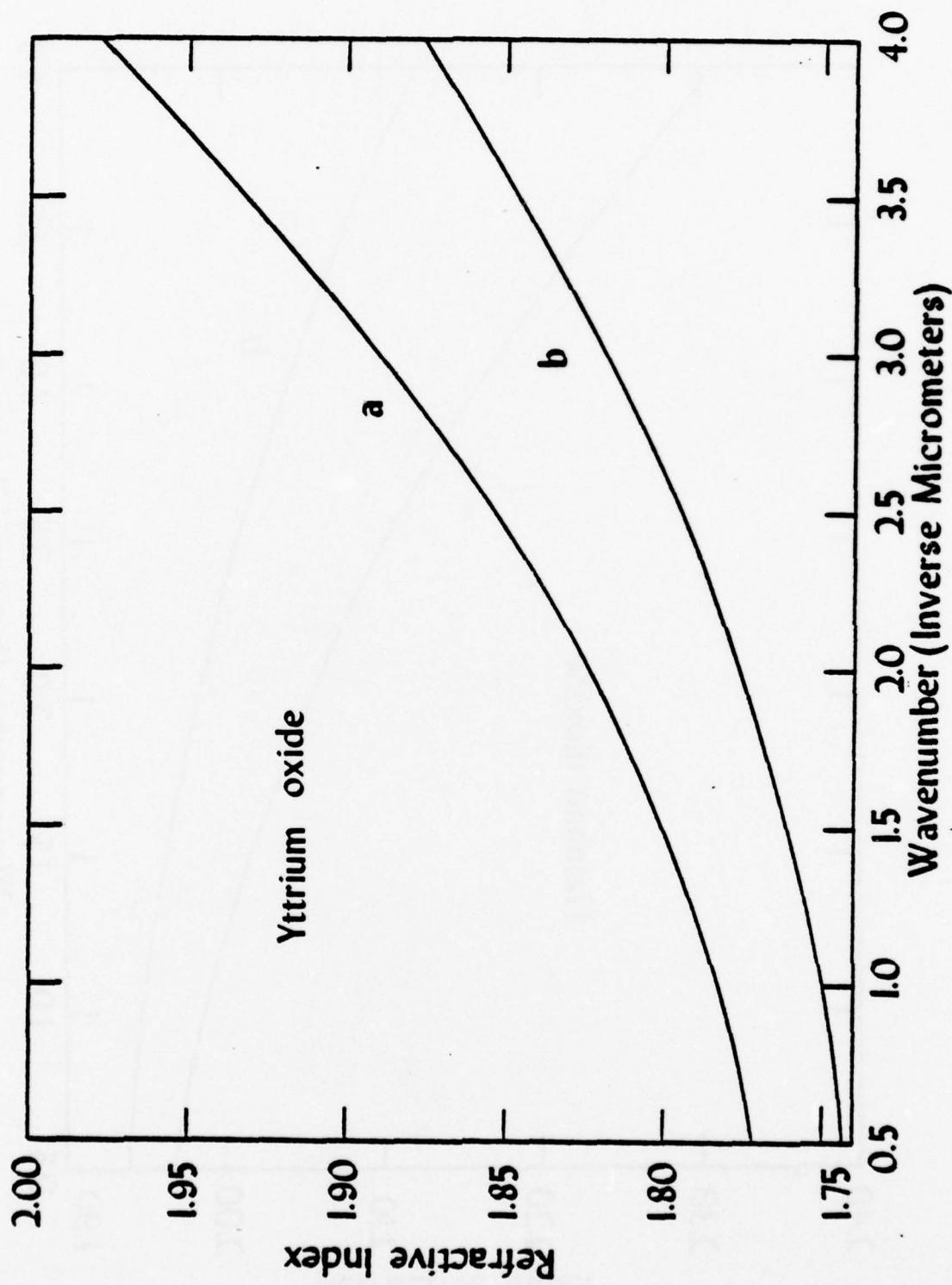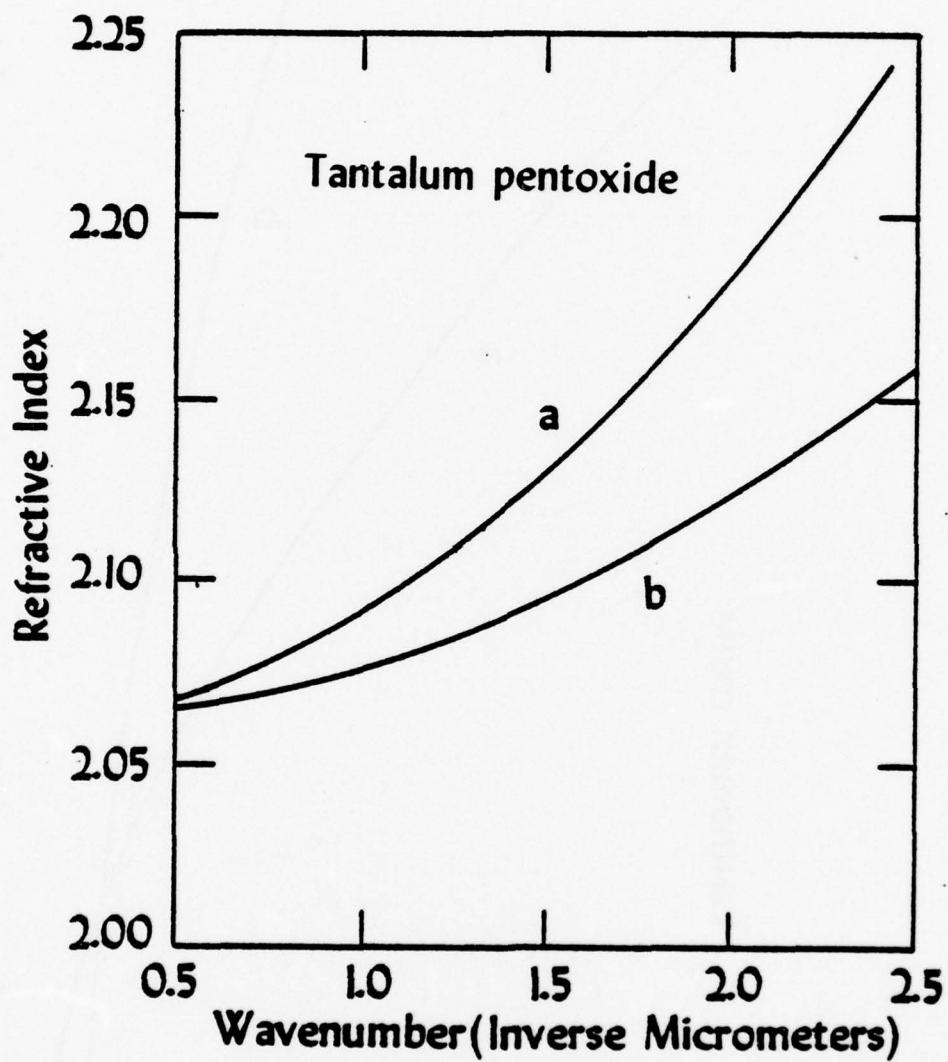
Fig.12
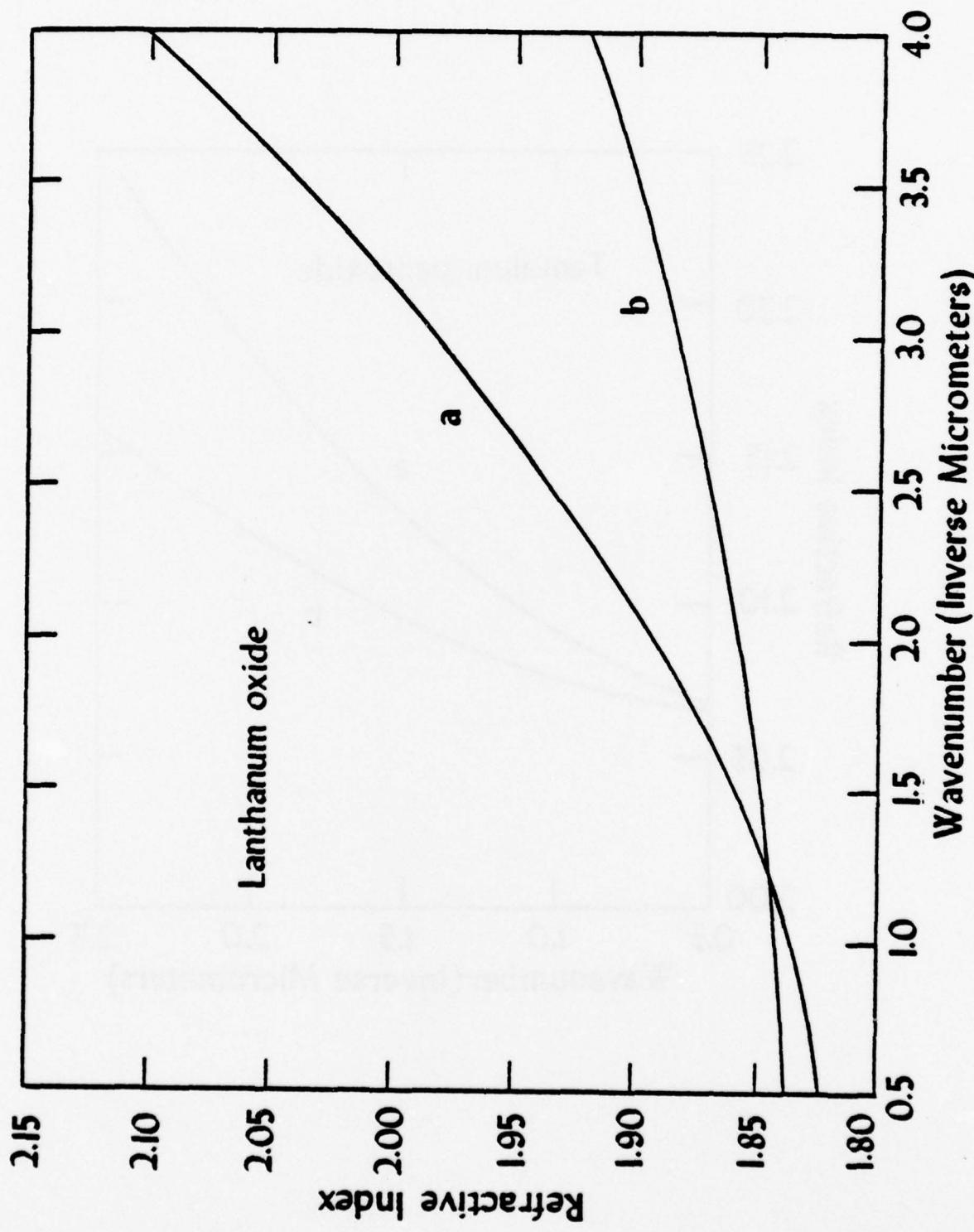
Fig. 13

the fact that both the A and the B coefficients are less for the post-baked sample than for the prebaked sample.

Finally, there is the question whether the baking for 14 hours at 400°C in air is the optimum treatment. There is evidence that a shorter bake does not fully oxidize the film. For example, Figures 14, 15 and 16 plot the refractive index of a hafnium dioxide film and two separate yttrium oxide films that were baked for four hours at 400°C in air. Comparing these data with those shown in Figs. 10 and 11, it is evident that the refractive index was changed relatively little by the four hour bake as compared to the unbaked sample.

A more vigorous baking of a sample at 700°C for four hours produced a considerable amount of crazing and cracking in the films. It is conjectured that this might be caused by the differential thermal expansion coefficient between the films and the relatively unexpansive silica substrate.

3.5 Extinction coefficient

The extinction coefficient $\underline{k}$ was determined from absoption measurements, as outlined in section 5.2. Due to the experimental uncertainty of $\pm 1\%$ in both $\underline{R}$ and $\underline{T}$, the absorption, and hence $\underline{k}$, could only be determined near 250 nm, as shown in Table 3-2. The lower absorption in the Y_2O_3, as compared to the HfO_2, is patent.

Table 3-2

Material	Prebake		Postbake	
	n	k	n	k
HfO_2	2.307	0.0156	2.2105	0.0218
Y_2O_3	1.9786	0.0043	1.8778	0.0065
La_2O_3	2.102	0.00111	1.920	0.00258

The extinction coefficient k and refractive index n of films as measured after evaporation and after baking at $400^{\circ}C$ for 14 h in air. The wavelength is 250 nm.

Figure 14

The computed refractive index for hafnium dioxide.
The broken curve corresponds to the postbake
measurement. The sample was baked for four h in air at
400°C.

Figures 15 and 16

The computed refractive index for two samples
of yttrium sesquioxide. Curve b is the postbake
measurement. The samples were baked at 400°C for four
h in air.

Hafnium dioxide

Refractive Index

Wavenumber (Inverse Micrometers)
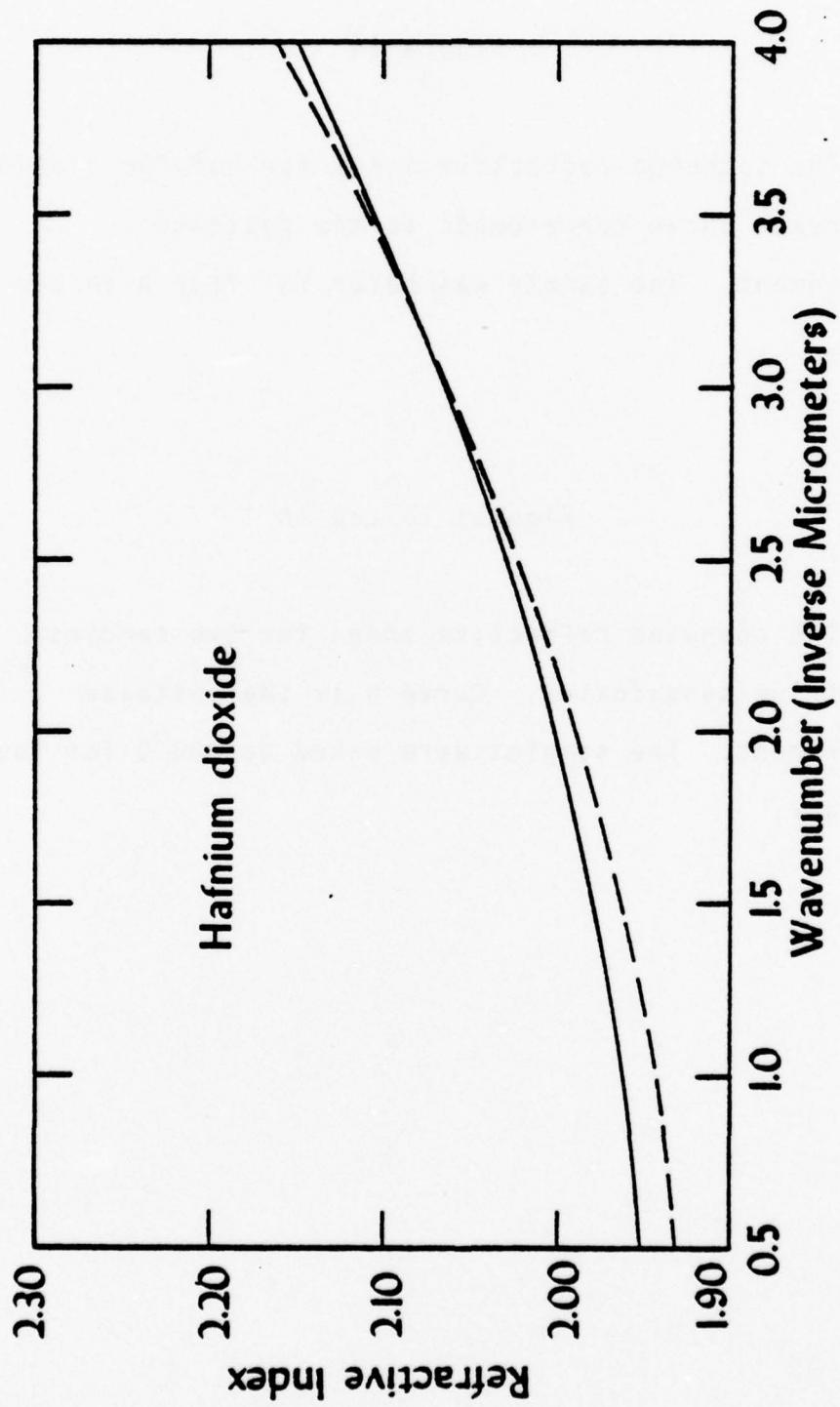
Fig. 14
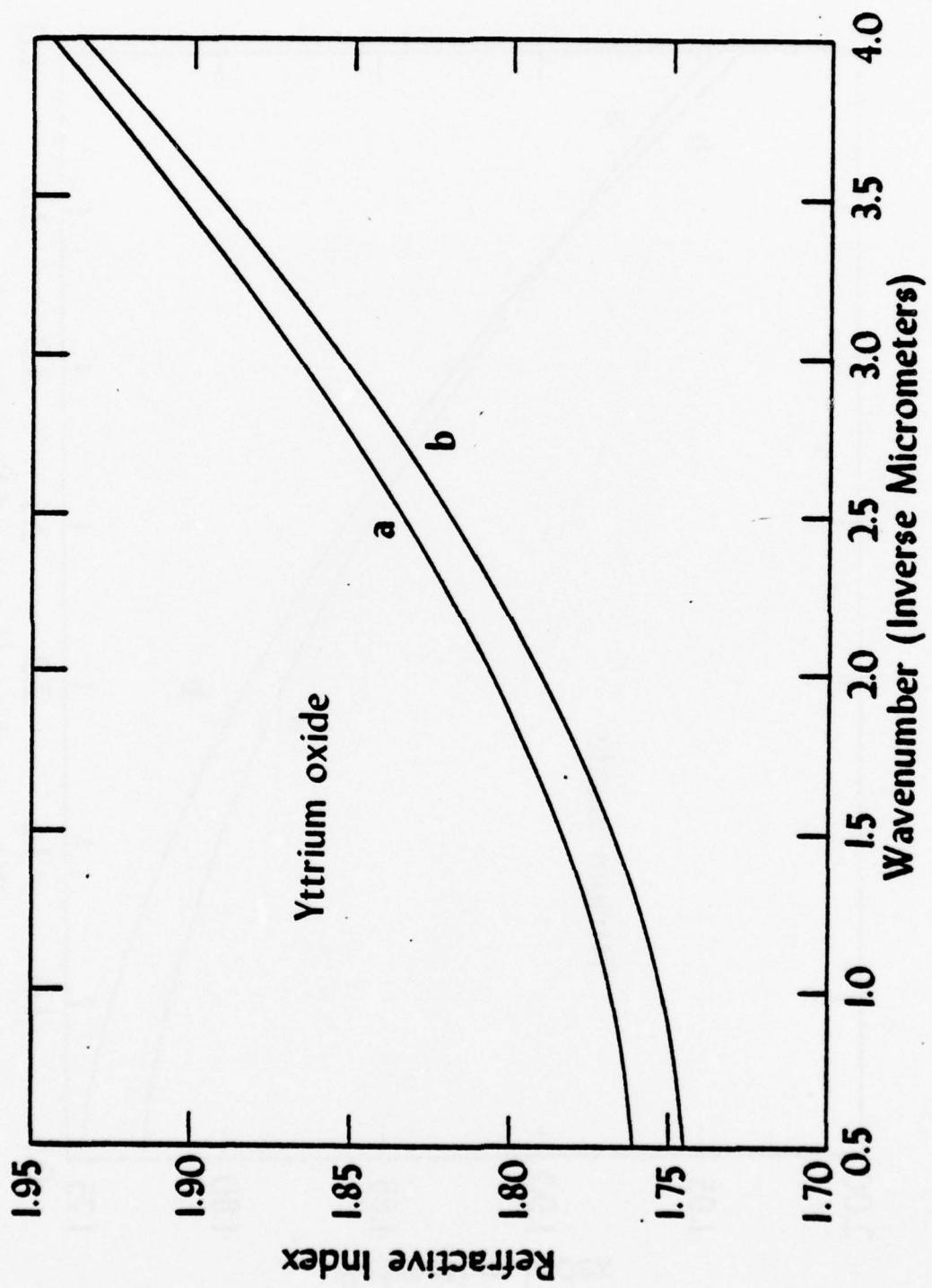
Fig. 15
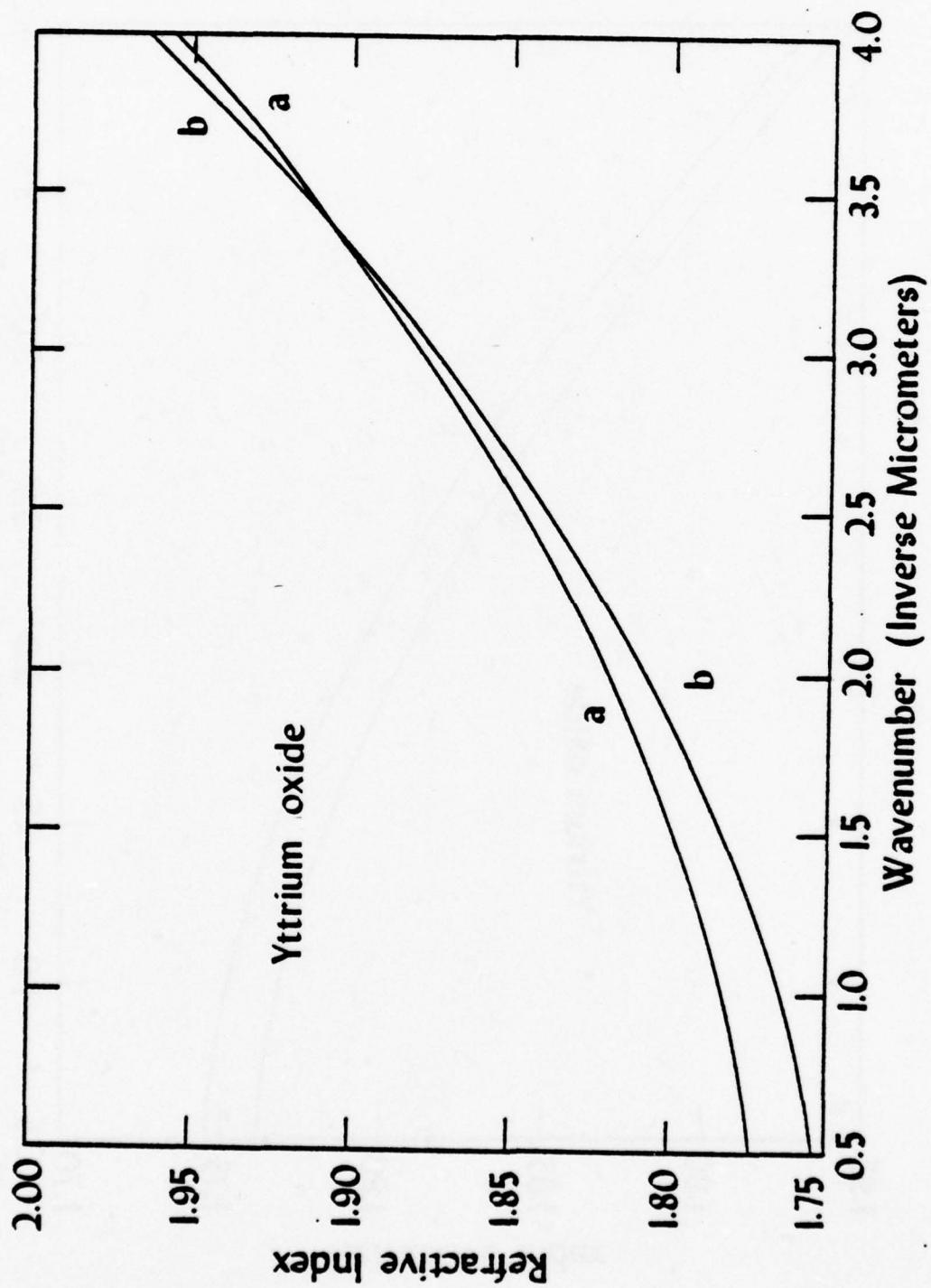
Fig. 16

3.6   Discussion of refractive index data

The determination of these refractive indices
points to some new ways to construct highly reflecting
laser damage resistant multilayer reflectors at 350 nm.
Consider, for example, the possible use of tantalum
pentoxide as a high index material. From the dispersion
polynomial, [Eq. (8)] the A and B coefficients in Table 3-1,
we find that the refractive index of baked tantalum pentoxide
is 2.19 at 350 nm. This means that seven alternate layers
of tantalum pentoxide and silica deposited upon a fused
silica substrate would produce a radiant reflectance of
94%. It is doubtful, however, that this reflectance
could be attained because of the absorption in the outer
layers of the tantalum pentoxide. This is ño deterrent,
however, because materials that have lower loss, such as
yttrium oxide and hafnium dioxide are now used in the
high index films at the top of the stack.

What are the advantages of using the tantalum
pentoxide for this total reflector? The chief advantage
is that the tantalum has little scatter and virtually no
mechanical stress. Furthermore, electron diffractographs
have shown that films of tantalum pentoxide are amorphous
and therefore the stack does not become rougher as more
layers are deposited. This technique of using a slightly
more absorbing but higher refractive index material at
the bottom of the total reflector means that the number

of layers and scattering of the stack will be lower, as
compared to a stack in which hafnium dioxide is used
exclusively as the high index layer.

4.   Properties of reflectors

    4.1   Introduction

        Multilayer dielectric reflectors at 250 nm
and 350 nm were prepared on a host of substrates --
fused silica, polished molybdenum, sputtered molybdenum,
and polished silicon carbide. Since these R and T data
are well summarized in another report [4], no effort is
made to reproduce the R and T curves of even a moiety of
the coatings that were produced under this contract.

    4.2   Reflectors at $\lambda = 350$ nm

        As an example of a reflector, Fig. 17 shows
the measured spectral reflectance of a multilayer of the
design

$$\text{air (H L)}^{11} \text{ H substrate}$$

where H and L represent, respectively, layers of hafnium
dioxide and silica of quarterwave optical thickness at
355 nm. The solid curve is the smoothed data measured at the
University of Rochester on a Cary model 14 spectroreflectometer.
The solid points are the measurements at Naval Weapons
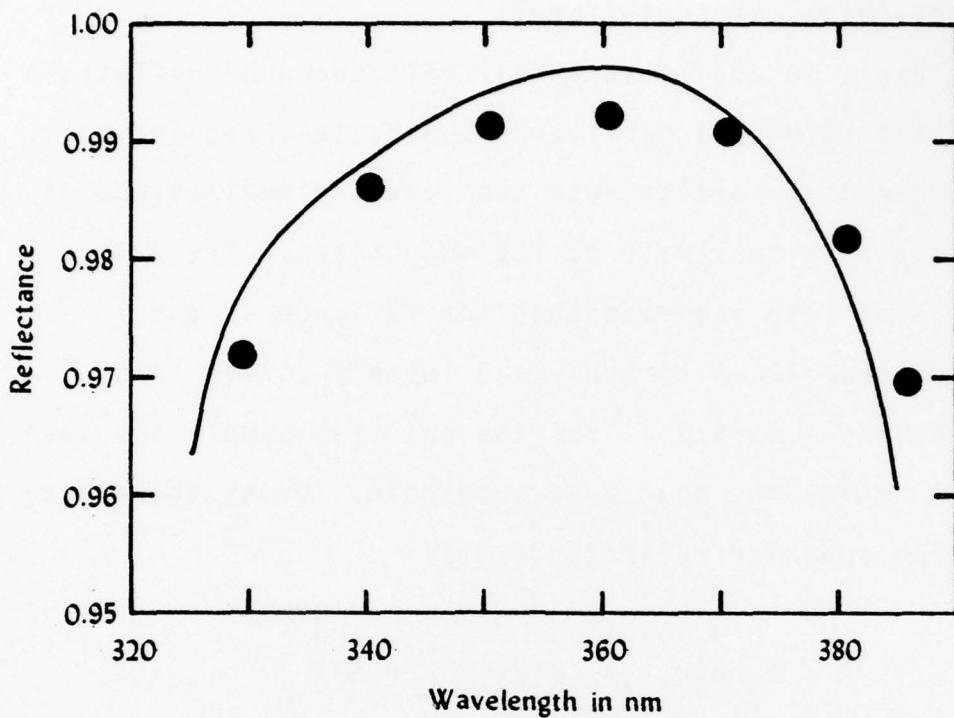
Fig. 17

The measured spectral reflectance of a multilayer of
the design

$$\text{air } (H\ L)^{11}\ H \text{ substrate}$$

where H and L represent, respectively, layers of hafnium
dioxide and silica of quarterwave optical thickness at 355 nm.
The solid curve is the smoothed data measured at the University
of Rochester on a Cary model 14 spectroreflectometer. The
solid points are the measurements at Naval Weapons Center,
China Lake, California.

Center, China Lake, California.

Figs. 18 and 19 show the reflectance of reflectors on sputtered Mo and massive Mo substrates, respectively. It is tempting to attribute the superior reflectance of the sputtered substrate to its smoothness. The data from China Lake indicate that the variance of the surface profile -- commonly and loosely called "rms roughness" -- is 4.7 nm for the polished sample and less than 1 nm for the sputtered substrate. Using these data, [5] the specular reflectance $\underline{R}$ is

$$R = R_o \exp(-(4\pi \sigma /\lambda)^2 = 0.973 \qquad (9)$$

for $\lambda = 355$ nm, $\sigma = 4.7$ nm and $R_o = 1.0$. Our measured reflectances exceeded this, but it can be argued that the measured biconical reflectance collected low-angle scattering and hence does not resemble the "specular" reflectance cited above.

4.3 Reflectors at 250 nm.

Figure 20 shows the reflectance of a 24 layer coating of the design:

$$\text{air (H L)}^{12} \text{ substrate}$$

where substrate is SiC. The H and L layers are HfO_2

Captions to Figs. 18 and 19

The measured reflectance of multilayers of the design

air $(H\ L)^{11}$ substrate

where H and L represent layers of quarterwave optical
thickness (at λ = 355 nm) of hafnium dioxide and silica,
respectively. The substrate is sputtered molybdenum
(Fig. 18) and polished Mo (Fig. 19).
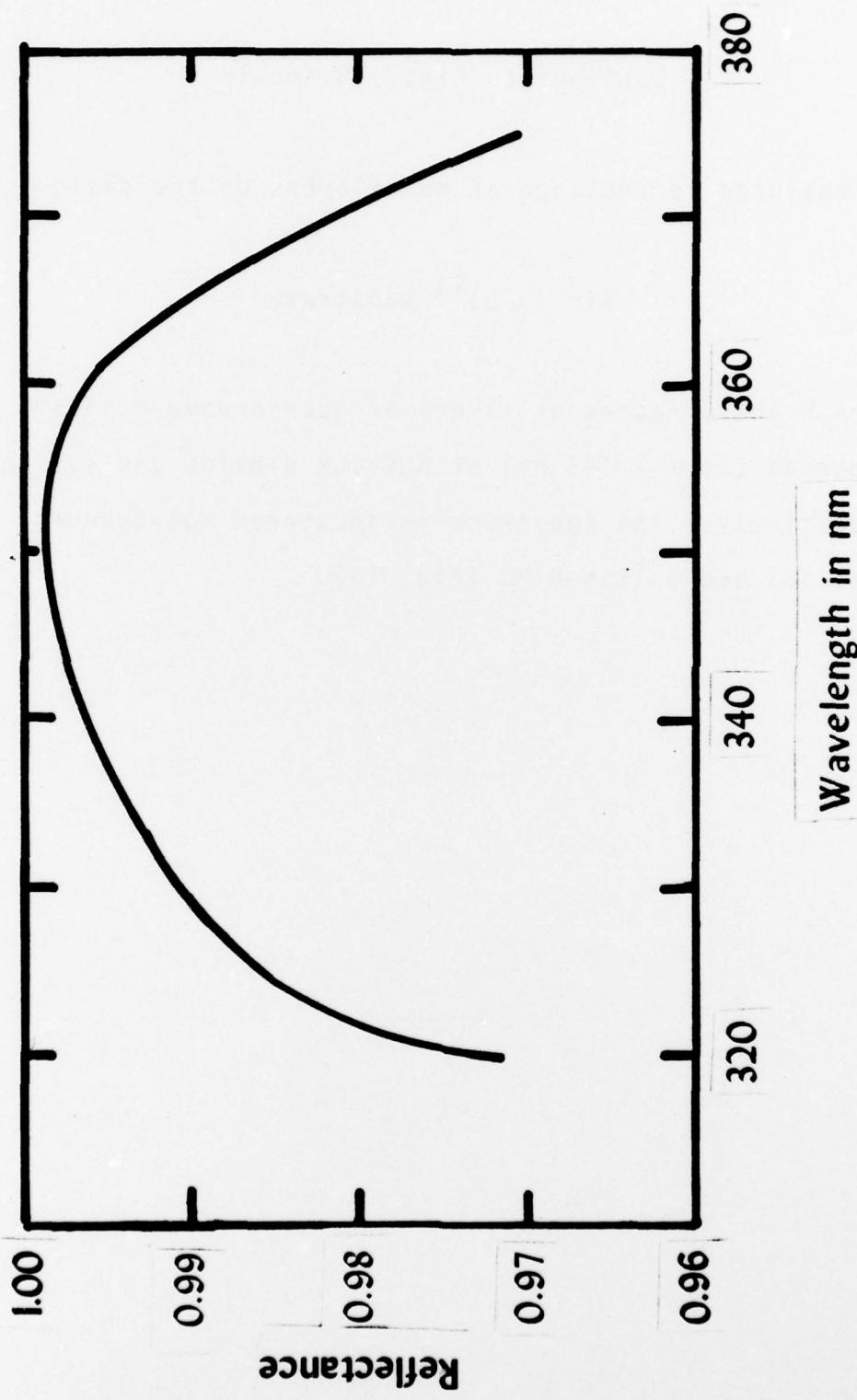
Fig. 18
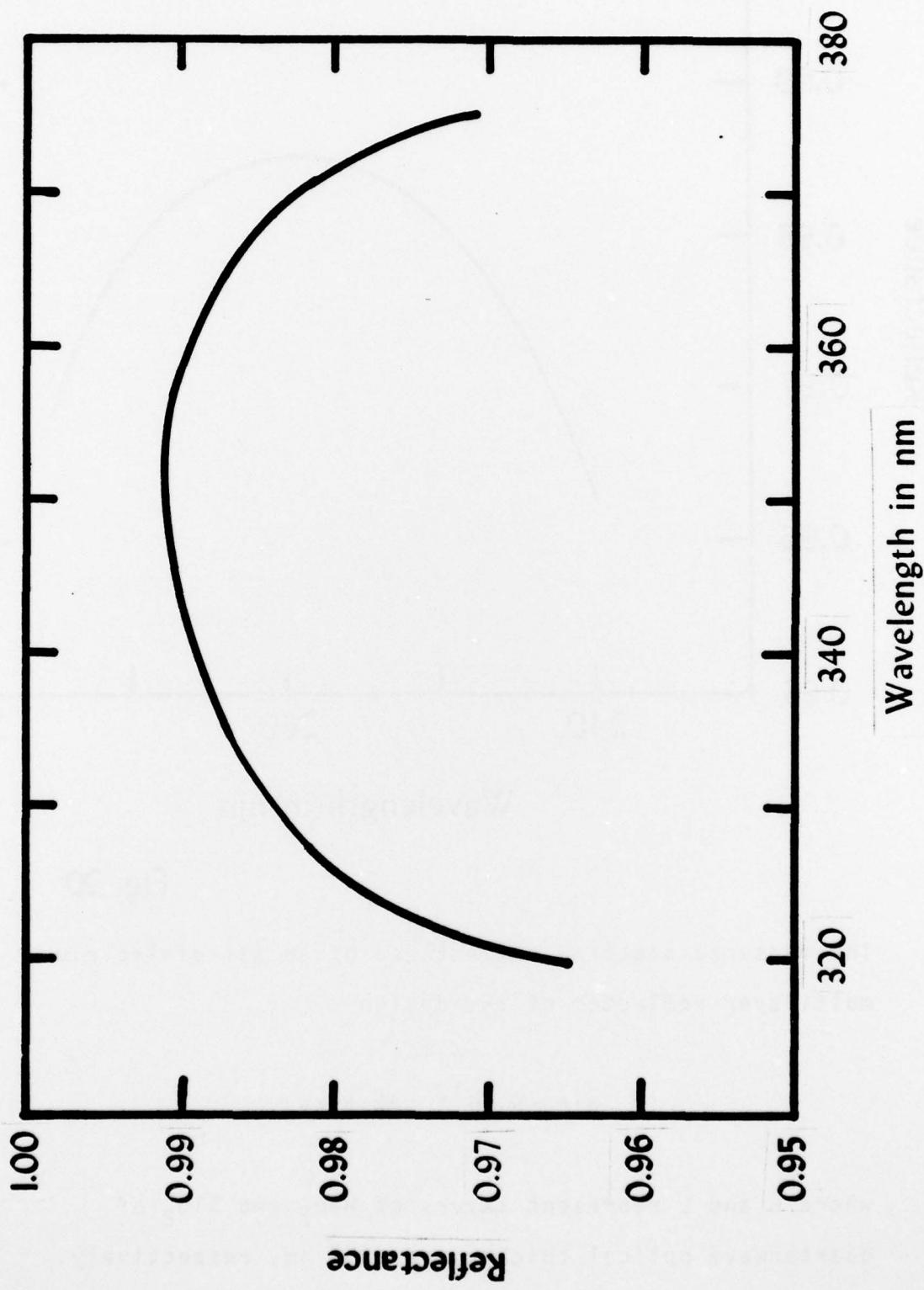
Fig. 19
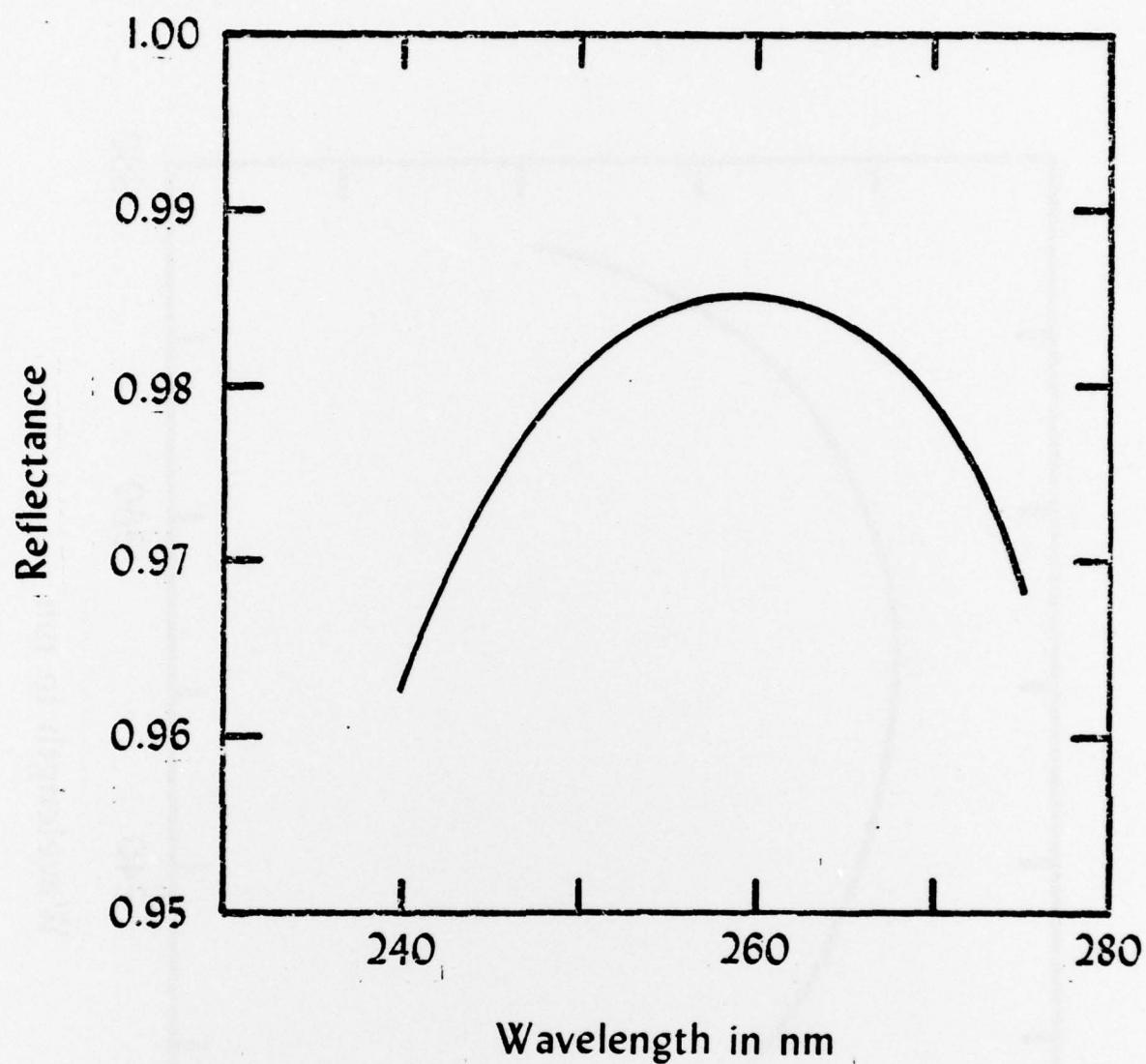
Fig. 20

The measured spectral reflectance of an all-dielectric
multilayer reflector of the design

$$air \ (H \ L)^{12} \ substrate$$

where H and L represent layers of HfO_2 and SiO_2 of
quarterwave optical thickness at 255 nm, respectively.
The substrate is silicon carbide.

and SiO_2, respectively. We assumed that the HfO_2 was
absorbing and hence the limiting factor in attaining
0.999 reflectance.

The first approach was to deposit a stack of hafnia
and silica, and then to overcoat it with a stack of yttria
and silica. The design was

$$air\ Y\ (L\ Y)^6\ (L\ H)^9\ substrate$$

where L is a low index layer of silica whose optical
thickness is approximately a quarterwave at 250 nm. Y and
H represent yttria and hafnia layers respectively, with
the same optical thickness as the silica. As shown in
Fig. 21, its reflectance is in excess of 99% at 250 nm.
The foregoing stack contains 31 layers.

There is strong evidence that the losses in the
layers at the top of the stack limit the reflectance.
For example, Figure 22 shows the spectral reflectance
of the design

$$air\ (Y\ L)^{17}\ Y\ substrate$$

where Y and L have the same meaning as in the previous
paragraph. This stack is composed entirely of yttria
and silica. As shown in Fig. 22, its peak reflectance is
approximately the same as that of the stack with the
hafnia on the bottom. In the absence of absorption, one
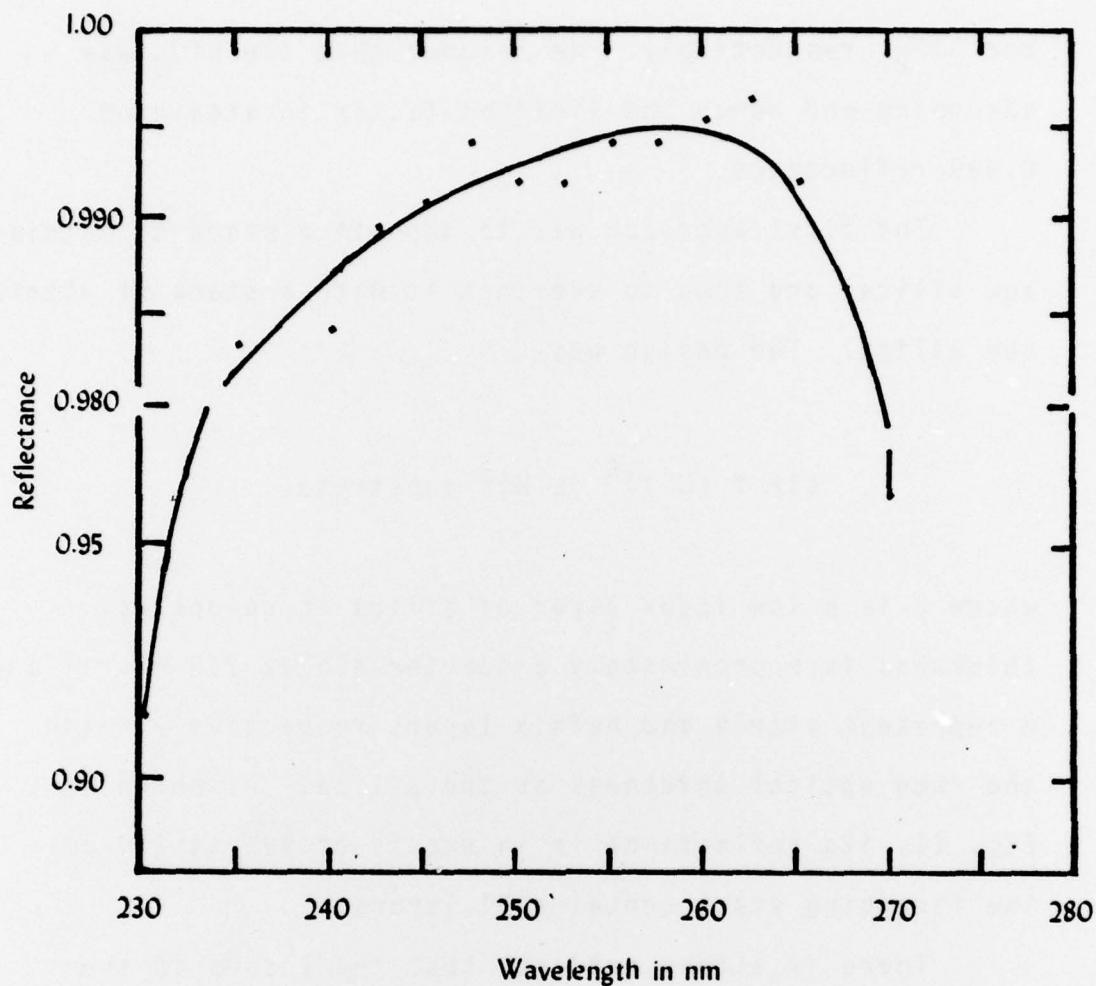
Fig. 21

The measured spectral reflectance (on a Cary model 14
spectroreflectometer) of a multilayer of the design

$$\text{air } Y \ (L \ Y)^6 \ (L \ H)^9 \text{ substrate}$$

where H, Y, and L represent layers of hafnia, yttria, and
silica, respectively, of quarterwave optical thickness at
250 nm. The ordinate changes scale at 0.98.
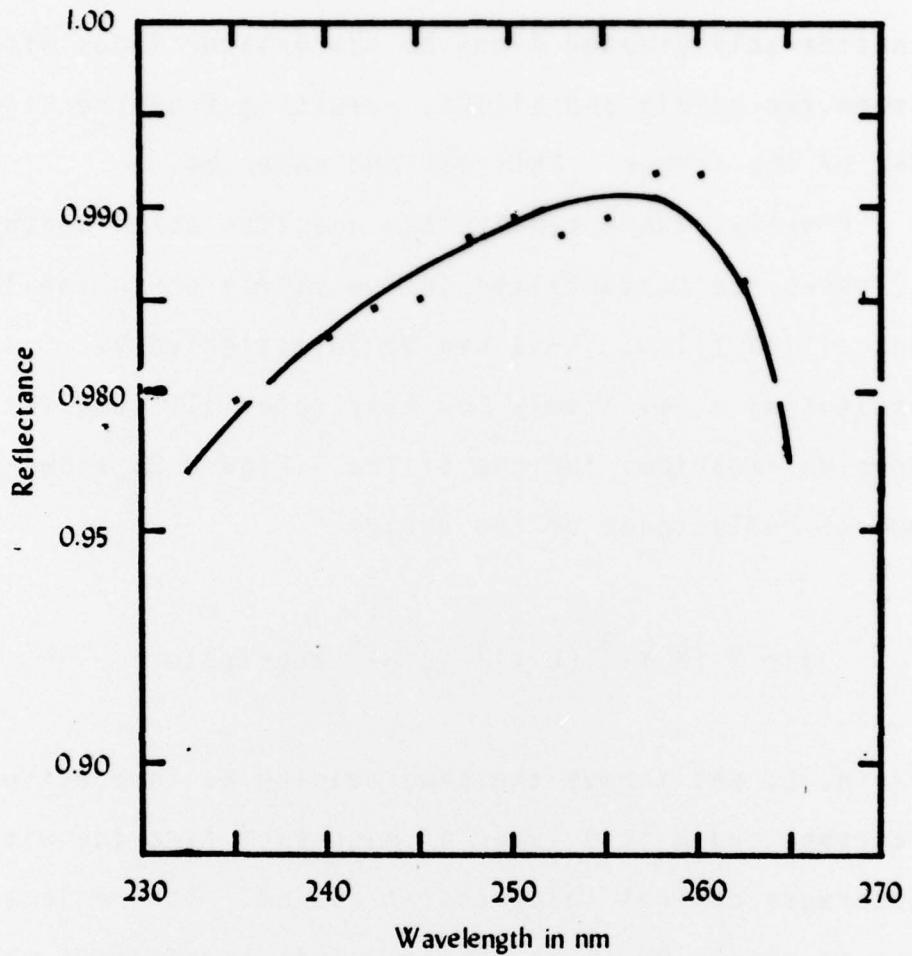
Fig. 22

The caption to Fig. 21 obtains, with the exception that the design of the multilyaer is

air Y (L Y)^{17} substrate

would expect that the stack with the hafnia should have a considerably greater R due to the greater index mismatch between the hafnia and silica, resulting from the higher index of the former. This was not observed.

Finally, there remains the question as to whether the losses are concentrated in the yttria or in the low index silica films. This can be investigated by substituting a relatively low loss material, such as magnesium fluoride, for the silica. Figure 23 shows the spectral reflectance of the design

$$\text{air } Y \ (M \ Y)^3 \ (L \ Y)^5 \ (L \ H)^9 \ \text{substrate}$$

where H, L, and Y have the same meaning as in previous paragraphs and M is a layer of magnesium fluoride with a quarterwave optical thickness at 250 nm. Its reflectance peaks at nearly 99.4% at 255 nm. This is evidence that the yttria is a major contributor to the absorption at 250 nm. The reason is that the index of the magnesium fluoride is considerably lower than the silica at this wavelength. For example, the MgF_2 index is 1.40 and the silica is 1.55. There is a considerably greater index mismatch between the magnesium fluoride and the yttria layers, which in turn produces a higher reflectance -- provided there are no absorption and/or scattering losses, of course. The fact that the reflectance of this type of stack is not appreciably different than one in which SiO_2
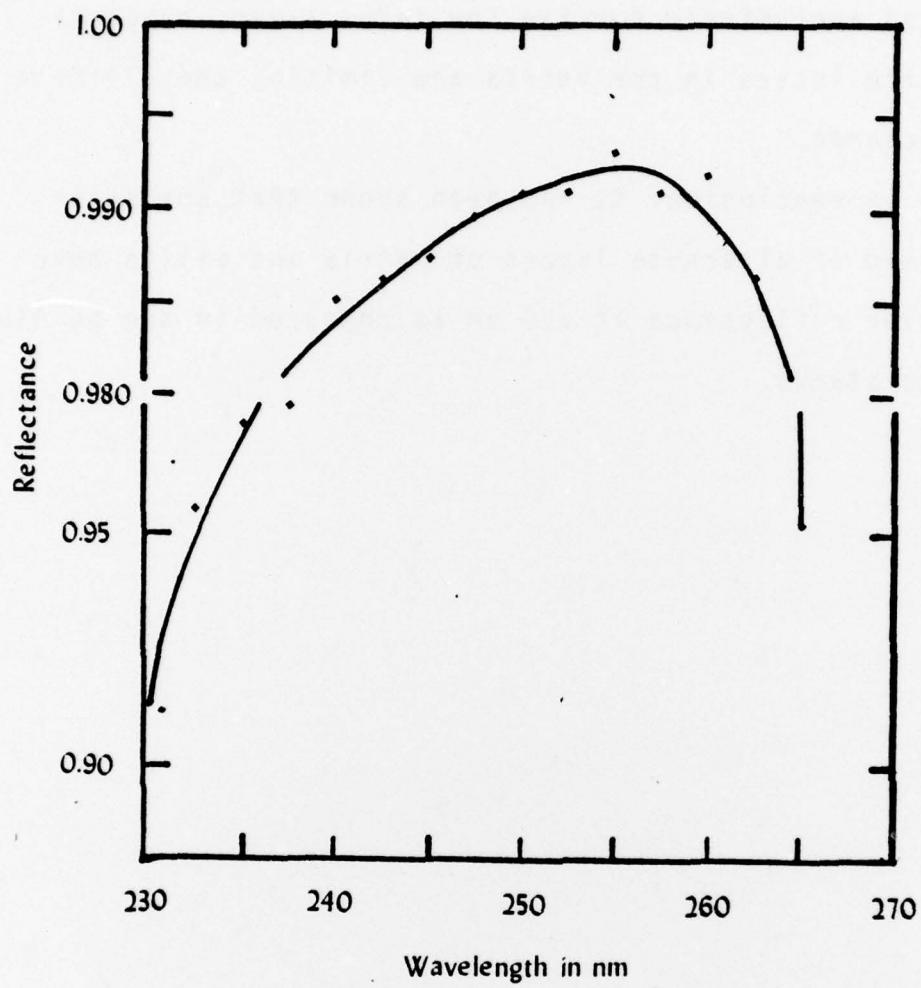
Fig. 23

The caption to Fig. 21 obtains, with the exception that the design of the multilayer is

$$\text{air } Y \text{ (M Y)}^3 \text{ (L Y)}^5 \text{ (L H)}^9 \text{ substrate}$$

H, L, and Y have the same meaning as in the caption to Fig. 21, and M represents a layer of magnesium fluoride whose optical thickness is a quarterwave at 250 nm.

is used exclusively for the low index layer, suggests that the losses in the yttria are limiting the ultimate reflectance.

In conclusion, it has been shown that the stacks composed of alternate layers of yttria and silica have superior reflectance at 250 nm as compared in the hafnia/ silica stacks.

5.   Appendices

5.1   Determination of the transmittance of the film
      via a double-beam ratio-recording spectrophotometer.

      Equation (1) cited in section 3.3 is an
approximation. Although it has appeared in the literature
[6,7], it is useful to rederive it in order to see if the
approximations are valid under the conditions of our usage.

An uncoated identical substrate is placed in the
reference beam. The notation is shown in Fig. 24. We
define:

T_s = Transmittance through the substrate/air interface

T_f = Transmittance of the evaporated layer

T_{ss}= Transmittance of the bare substrate

T_{fs}= Transmittance of film and substrate

T_m = Transmittance, as measured on the ratio-recorder

R = Reflectance of substrate/air interface

R_f = Reflectance of the evaporated film at the
        film/substrate interface

A = Absorption in the evaporated film

The transmittance measured on the dual-beam ratio
recorder is

$$T_m = \frac{T_{fs}}{T_{ss}} \ . \qquad\qquad (10)$$

uncoated
substrate

R T_s T_{ss}

coated
substrate

T_f R T_s T_{fs} R_f
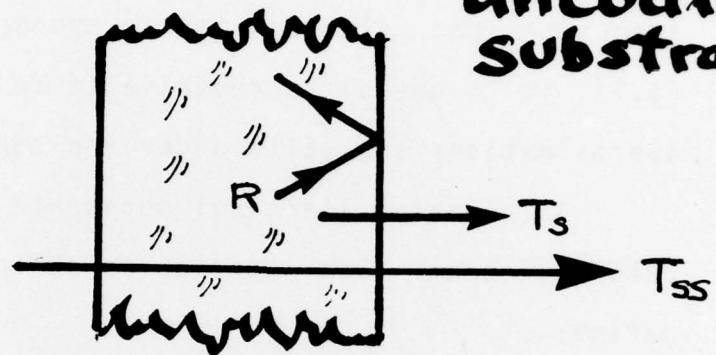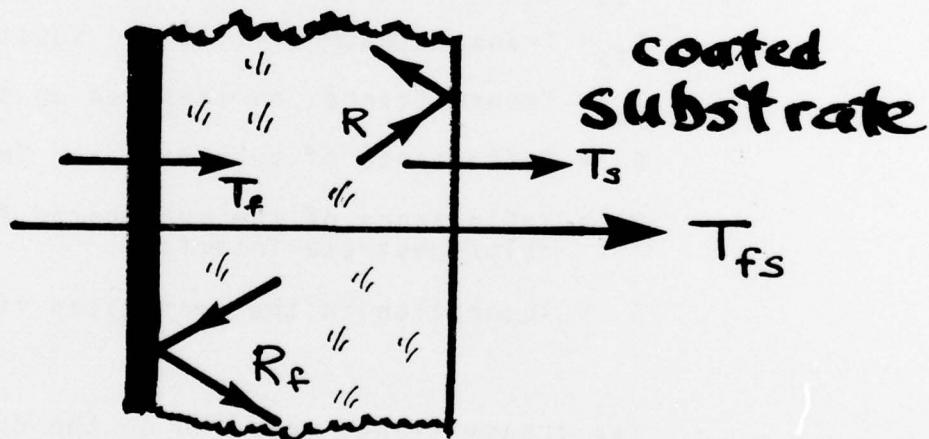
Fig 24

For a nonabsorbing substrate

$$T_{ss} = \frac{T_s^2}{(1 - R^2)} \tag{11}$$

$$T_{fs} = \frac{T_f T_s}{(1 - R_f R)} \quad . \tag{12}$$

Ergo:

$$T_m = \frac{T_f T_s / (1 - R_f R)}{T_s T_s / (1 - R^2)} \tag{13}$$

which reduces to

$$T_m = \frac{(1 + R) T_f}{(1 - R_f R)} \quad . \tag{14}$$

Using the identities

$$T_s = 1 - R, \tag{15}$$

$$T_f = 1 - R_f - A, \tag{16}$$

where A is the radiant absorption of the film, we find

$$T_f = \frac{T_m [1 + R(A - 1)]}{1 + R(1 - T_m)} \quad . \tag{17}$$

If A << 1, then Eq. (1) obtains:

$$T_f \cong \frac{T_m(1 - R)}{1 + R(1 - T_m)} \quad . \qquad (18)$$

5.2 The determination of the extinction coefficient k from the radiant absorption

The film of metric thickness $\underline{h}$ with optical constant $\hat{\underline{n}} = \underline{n} - \underline{j}\,\underline{k}$ is deposited upon a substrate of index $\underline{n}$. The absorption $\underline{A}$ is defined in Eq. (17). When flux impinges upon the layer from the incident medium of index $\underline{n}_o$, the $\underline{A}/\underline{T}$ ratio is

$$\frac{A}{T} \cong \frac{k\left[(n^2 - n_s^2)S + \gamma(n^2 + n_s^2) + kn_s(2(C - 1) + \gamma^2)\right]}{2\,n_s(n^2 + k^2)} \qquad (19)$$

where γ is double the phase thickness of the layer

$$\gamma = 2\beta \qquad (20)$$

$C \equiv \cos\gamma$, and $S \equiv \sin\gamma$. is defined in Eq. (7). Equation (19) is precise in the expansion of the exponential function $\underline{\exp}\,(\underline{x})$ into terms of order $\underline{x}^2$.

It does not depend upon the refractive index $\underline{n}_o$ of the indicent medium, since $\underline{A}/\underline{T}$ is related to the "net flux ratio" and depends only upon the admittance of the medium on its emergent side. When the quadratic terms in $\underline{k}$ are ignored and the optical thickness is either a quarterwave or a halfwave, $\underline{A}/\underline{T}$ is directly proportional to the layer thickness.

6. References to the literature

1. P. Baumeister and O. Arnon: "Use of hafnium dioxide in multilayer dielectric reflectors for the near uv," Appl. Opt. 16, 439 (1977).

2. G. Hass, J.B. Ramsey, and R. Thun: "Optical Properties of various evaporated rare earth oxides and fluorides," J. Opt. Soc. Am. 49, 116 (1959).

3. E. Ritter: "Dielectric Film Materials for Optical Applications," in Physics of Thin Films, G. Hass, M. Francombe, and R. Hoffman, eds., (Academic Press, N.Y., 1975), Vol 8.

4. H. Bennett, A. Baer, R. Hughes, V. Rehn, J. Stanford: Ultraviolet components for high energy applications. US Naval Weapons Center Report NWC TP 6015 (March 1978).

5. H.E. Bennett and J.O. Porteus: "Relation between surface roughness and specular reflectance at normal incidence," J. Opt. Soc. Am. 51, 123 (1961).

6. H.E. Bennett and Jean M. Bennett: "Precision Measurements in Thin Film Optics," in Physics of Thin Films, G. Hass, M. Francombe, and R. Hoffman, eds. (Academic Press, N.Y., 1972), Vol 4.

7. J.M. Bennett, E.F. Ashley: "Calibration of instruments measureing reflectance of transmittance," Appl. Opt. 11, 1749 (1972).